The University of Kitakyushu

Doctoral Thesis

Study on controlling factors of air pollution in northern part of Kyushu, Japan – Transboundary transportation and local meteorology condition –

Yuan PENG

Graduate Programs in Environmental Systems

Content

Abstract This study investigated the effects of transboundary transport and local meteorological conditions on air quality in Kitakyushu, the northern part of Kyushu, Japan. The presence and sources of anthropogenic/non-sea-salt inorganic chloride (nss-Cl) in ambient air were studied at the survey site, a suburb of Kitakyushu. By applying the four-stage filter pack system, samples (both particulate matter and gaseous species) were collected daily (24-hour sampling) over one year (December 2016 to November 2017). Anthropogenic/nss-Cl concentrations were generally low and were detectable for only 263 days (approximately 72% over one year). Anthropogenic/nss-Cl concentrations above 20 $nmol \cdot m^{-3}$ were observed over 50 days, and the 72-h backward trajectory results suggest a strong correlation with transboundary transport in the west/northwest rather than with domestic/local emissions from waste incineration, coal combustion, and volcanic eruptions. The PSCF and CWT results indicate that northeastern and southern China, Mongolia, Russia, and the Sea of Japan were important potential source areas for anthropogenic nss-Cl at the survey site.

On the other hand, the atmosphere's stability is an essential parameter in controlling air pollution. This study monitored local air pollution problems by measuring atmospheric methane concentrations. Methane concentrations around urban and suburban areas were also investigated based on (1) CH_4 fluxes/emissions, (2) vertical profiles of air temperature, and (3) land use. Methane fluxes/emissions from automobiles were not ignored in the heart of industrialized cities, although it was not a significant contributor globally; in addition, the contribution of landfills related to wind direction. In contrast, CH_4 fluxes/emissions were a mixture of CH_4 from automobiles and rice paddies in suburban areas. The atmosphere in the urban center area was stable at ca. 200 m, during daytime and even in the summer; this elevated

temperature inversion layer prevented air pollutants and the air itself from vertical mixing/diffusion/transportation; meanwhile, the atmosphere in the suburbs formed the grounded temperature inversion layer at night in the summer. Interestingly, it was not formed in winter all day, likely because of the strong wind velocity due to the monsoon. Land use also influenced the CH_4 concentrations; especially in suburban areas, where rice fields remained undeveloped. The CH_4 concentrations increased significantly from midnight to early morning in summer, while the atmosphere was stable.

Chapter 1 Introduction

1.1 Air quality and air pollution

Air is the gas that surrounds the earth and maintains the survival of humans and living things. The troposphere, or air layer within 12 kilometers of the ground, is critical to the existence of people and other living things. It comprises 78.1 % nitrogen, 21% oxygen, 0.9 % argon, and the remaining contaminants. A clean atmosphere is one of the necessary conditions for human survival. In five weeks without food or five days without water, a person can still maintain life. However, it takes only a few minutes without breathing air to die. According to the American Lung Association (ALA), adults consume 2,000 gallons (7,570 liters) of air per day (ALA, 2017). The atmosphere has a specific self-purification ability due to natural processes and other pollutants in the atmosphere by the atmospheric self-purification process from the atmosphere to remove to maintain a clean atmosphere.

Air quality reflects air pollution, which is judged based on the concentration of pollutants in the air. Air pollution is a complex phenomenon, and many factors influence the concentration of air pollutants at a given time and place. The magnitude of anthropogenic pollutant emissions from stationary and mobile sources is one of the most critical factors affecting air quality, including exhaust from vehicles, ships, aircraft, industrial pollution, residential living and heating, waste incineration, etc. Previous studies have proven that the world faces many environmental problems today, such as the greenhouse effect, the ozone hole, forest degradation, the spread of acid rain, land desertification, water pollution, and the reduction of biodiversity and genetic diversity (Cameron et al., 2013; Zscheischler et al., 2014; Zhang et al., 2018;

Grennfelt et al., 2020; Zhang et al., 2020).

With rapid socio-economic growth and industrialization, human-caused air pollution has become increasingly severe, especially in cities with high concentrations of factories, automobiles, and people. Air pollution threatens human's daily life, endangers human health, inconveniences people's work, and affects or endangers the survival of various organisms and damages equipment, buildings, etc. directly or indirectly.

Air pollution has become one of the most severe environmental health threats worldwide. Seven million deaths in 2012 (1/8 of all global deaths) were associated with exposure to air pollution (WHO, 2016). Approximately 7 billion people (92% of the global population) live in areas that exceed the World Health Organization's (WHO, 2012; 2021) annual air quality guidelines for $PM_{2.5}$, and 3.6 billion people (47% of the global population) are exposed to household air pollution due to the use of solid fuels for cooking (Jerrett et al., 2009). Recent studies have also shown that even low levels of air pollution, below current WHO guidelines and most national standards, can affect cardiovascular health (Strak et al., 2017; Pappin et.al., 2019). In addition, climate change is leading to an increase in the frequency and severity of wildfires, which is leading to large-scale smoke episodes and associated health effects affecting major metropolitan areas (Conover, 2001; Reid et.al., 2016).

On the other hand, Asia is a relatively underdeveloped region in the world, with a large population and slow development. In order to accelerate economic development, each country has exploited nature in a big way, and the use of resources is relatively large, but at the same time, the effective utilization of resources is not high, the treatment of energy waste is not appropriate and adequate, and the impact of environmental pollution on society and human

beings is not clear enough. As a result, we have not only lost a lot of energy, but also brought a lot of pollution to the environment, especially air pollution.

When air quality is good, the air is clear and contains only small amounts of solid particles and chemical pollutants. Poor air quality, which contains high pollutants, is often hazy and dangerous to health and the environment. Air quality is described according to the Air Quality Index (AQI), which is based on the concentration of pollutants present in the air at a particular location. In Japan, after 1955, the city of Yokkaichi was covered with sulfuric acid fog, and in 1964, the citizens of the city suffered from asthma attacks and some died from asthma. With the joint efforts of the Japanese government and people, the air quality is now getting better. The AQI for the whole country is between 0 and 50, with an average of around 30. The AQI was introduced as a summary index by the United States Environmental Protection Agency (USEPA) in 1998, and the construction of the AQI provides a means to distinguish between “good” and “unhealthy” air quality (Kowalska et al., 2009; Perlmutt and Cromar, 2019). This means that the air can be breathed without any risk to health. However, there are some places where pollution levels are higher than usual, such as Tokyo or Osaka. Kyushu has a number of industrial plants that produce pollutants such as sulfur dioxide, nitrogen oxide, carbon monoxide, and particulate matter. These pollutants have been found in many parts of Japan including Tokyo, Kyoto, Osaka, and Nagoya. In addition to these major sources, there are also smaller factories producing lead compounds which can cause health problems if inhaled over long periods of time. There are also a number of coal-fired power stations located around Kyushu that release large amounts of dust into the atmosphere causing haze during summer months when they operate at full capacity. Japanese government has implemented the Air

Pollution Control Law in 1968 (Ministry of the Environment, 2010) to control the national environmental quality. Other comprehensive policy approaches combined with energy-related topics were launched later to mitigate environmental pollution while maintaining the national economic growth. Four issues, water, air, soil and noise, are the most significant factors in the Japanese environmental quality standards, and the air quality standards for the aim target pollutant, air pollution, are given in Table 1. The air environment in Japan is very different from that of western countries. It has a lot of natural disasters, such as earthquakes and typhoons. The temperature changes are also big, because of their location between the ocean and mountains. The climate is mild, with a mean temperature of 9.9°C (49.6°F) and an annual average relative humidity of about 55%. About 60% to 70% of the rainfall occurs between June and September, while snowfall is rare except in Hokkaido. Average daily maximum temperatures range from 22.7°C (73°F) in July to 6.5°C (43°F) in January. In general, Japan has four seasons: spring (March, April, and May), summer (June, July, and August), autumn (September, October, and November), and winter (December, January, and February).

Table 1. Environmental quality standards of atmosphere in Japan

Substance	Environmental conditions
SO_2	The daily average for hourly values shall not exceed 0.04 ppm, and hourly values should not exceed 0.1 ppm.
CO	The daily average for hourly values shall not exceed 10 ppm, and average of hourly values for any consecutive eight hour period should not exceed 20 ppm.
SPM	The daily average for hourly values shall not exceed 0.10 mg/m^3, and hourly values should not exceed 0.20 mg/m^3.
NO_2	The daily average for hourly values should be within the 0.04–0.06 ppm zone or below that zone.
O_X	Hourly values should not exceed 0.06 ppm.
Benzene	Annual average should not exceed 0.003 mg/m^3.
Trichloroethylene	Annual average should not exceed 0.13 mg/m^3.
Tetrachloroethylene	Annual average should not exceed 0.2 mg/m^3.
Dichloromethane	Annual average should not exceed 0.15 mg/m^3.
Dioxins (PCDDs, PCDFs and coplanar PCBs)	Annual average should not exceed 0.6 pg-TEQ/m^3.
Fine particulate matter ($PM_{2.5}$)	The annual standard for $PM_{2.5}$ is less than or equal to 15.0 μg/m^3. The 24-h standard, which means the annual 98th percentile values at designated monitoring sites in an area, is less than or equal to 35 μg/m^3*.

*: Source from the website, Environmental Quality Standards in Japan - Air Quality

1.2 The main factors affecting air quality

Air pollution is a growing problem worldwide and is problematic because it varies from place to place, influenced by meteorological, topography, pollutant emissions, transboundary transportation, atmospheric reactions, and deposition. Air pollution exists globally, affects the lives and health of 90% of the global population, and exhibits different seasonal and diurnal variations across geographic regions (WHO, 2018). Local emissions of pollutants and transboundary transport of pollutants, such as exhaust from cars and ships, industrial pollution, and waste incineration, are among the most important variables affecting air quality. The density of urban development, topography and meteorology are also important factors affecting air quality.

Air pollution has a significant effect on places near its source, but because it can travel so far in the atmosphere, air pollution generated in one place can also affect places far away. For example, Smith et al. (2015) estimated that marine vessels are responsible for approximately 13% of global anthropogenic sulfur dioxide (SO_2) emissions, while Zhang et al. (2017) estimated that about 12% of total premature deaths from fine particulate matter ($PM_{2.5}$) are caused by transboundary air pollutants. Yin et al. (2021) research show that transboundary transport of air pollution from South and Southeast Asia was associated with the high concentrations of most air pollutants observed in Southwest China. Similarly, Chuang et al. (2020) determined that average air pollution levels are influenced by $PM_{2.5}$ transported by seasonal winds from neighboring regions. The transboundary transport of air pollutants in the East Asian region has become a serious concern in recent years. Air pollutants emitted from urban and industrial areas in China, Korea, and Japan travel long distances and pass to

negatively impact plants and humans in downstream regions (Lee et al., 2008; Wang et al., 2013). Regional aerosol size distributions are influenced directly by primary particles transported over long distances, such as yellow sand and black carbon (Kulmala et al., 2004; Weber et al., 2003).

Although the long-range transport of air pollutants can lead to air pollution in a region, the sources of pollution near a region remain a significant determinant of local air quality. Pollutants such as nitrogen dioxide (NO_2) and sulfur dioxide (SO_2) are most concentrated near their sources (transportation, energy production, and industry), and this occurs mainly in urban and industrial areas (Yang et al., 2018; Zhou et al., 2021). Previous studies suggest that this is due to urban areas' significant and sustained development, affecting local air quality (Cheng et al., 2017; Li et al., 2019; Udemba et al., 2020). From 2016 to 2017, traffic emissions accounted for a considerable percentage of fine particles ($PM_{2.5}$) in Beijing, accounting for 5–12 percent of primary $PM_{2.5}$ (Srivastava et al., 2021; Xu et al., 2021). Secondary particles are also produced by road traffic as a result of gas-to-particle transition (Pant and Harrison, 2013; Harrison et al., 2021b). Anthropogenic emission sources such as motor vehicles, road dust, and cooking odors significantly increase $PM_{2.5}$ and gas precursors in metropolitan areas (Huang et al., 2014; Pandey et al., 2014). Furthermore, the density of structures in urban locations can change the surface albedo, resulting in a higher heat island effect than in suburban settings (George et al., 2007; Sailor and Fan, 2002).

Atmospheric conditions (e.g., wind) can affect the dispersion of pollutants and are highly variable. Strong winds make long-distance transport possible, while windless environments can cause pollutants to accumulate. Large cities in subtropical and tropical regions can experience

severe pollution events due to very little wind and many hours of sunlight. Temperature can also affect air quality. In urban areas, air quality is often worse in the winter months. When the air temperature is more relaxed, exhaust pollutants can be trapped close to the surface beneath a layer of dense, cold air. In the summer months, heated air rises and disperses pollutants from the Earth's surface through the upper troposphere, and increased sunlight results in more harmful ground-level ozone. Local meteorological factors, such as land and sea breezes near mountains and towns, also influence pollution dispersion and secondary pollutant generation. For example, local climatic conditions tend to intensify or abate their impacts depending on locations and seasonal factors (Goyal et al., 2021). Meteorological extremes, such as severe storms and gales, and near-surface events such as dust storms, also have substantial impacts on air quality (Ashrafi et al., 2017; Tian et al., 2021). Moreover, many areas are periodically subjected to complex atmospheric conditions, including temperature inversion layers and thermal updrafts that can restrict or accelerate the dissipation of pollutants (Murthy et al., 2020).

1.3 Location of Kitakyushu City

Kitakyushu is a government-designated city in the northern section of Japan's Fukuoka Prefecture. It is located at the northernmost point of Kyushu Island, across the Kanmon strait from Honshu, being located on the forefront of transboundary transportation from the Asian landmass. Kitakyushu city, with a population of 940,978/492 km^2 (Kitakyushu City, 2019), is one of the famous industrial cities in Japan. Kitakyushu City is bordered by the Sea of Japan to the north and the East China Sea to the west. The central part of Kitakyushu City is mostly hilly, including the Hiraodai (lit. Flat Tail Plateau) karst plateau, Mount Adachi and Mount Sarakura.

Moreover, Mt. Sarakura is famous as one of Japan's new top three night scenes. Furthermore, Sarakura is close to Kitakyushu University Hibikino campus, ca. 8 km. The University of Kitakyushu Hibikno campus is in Wakamatsu-Ku (located in the suburbs of Kitakyushu City). The university is comprised of two campuses, Kitagata and Hibikino. The Hibikino campus and several other scientific institutes are located in the Kitakyushu Science and Research Park.

The coastal areas of Kanmon Strait and Hibiki Nada in Kitakyushu City have a Pacific climate. In winter, Kitakyushu is cloudy due to the influence of convective clouds in the Sea of Japan, but the precipitation is much less than the coastal areas of the Sea of Japan. Spring is the time of the year when the temperature in Kitakyushu varies greatly. Daylight hours gradually become longer in the late spring. Although summer in Kitakyushu is hot, the average temperature is slightly lower than inland cities due to Kitakyushu's northern location and being close to the coast. In addition, the weather in the summer is quite consistent. Precipitation throughout the year is also concentrated in summer. Kitakyushu is susceptible to typhoons in September, which is also a period of heavy rainfall. After entering October, with the strengthening of high pressure forces, Kitakyushu enters autumn, and the weather is mostly sunny. In terms of marine meteorology, Hibiki Beach is part of the Sea of Japan, and the wind speeds and waves are larger in winter.

Located at the intersection of Honshu and Kyushu, Kitakyushu City is also a transportation hub, extending in all directions by land, sea and air. There are many cars in Kitakyushu City, but public transportation such as JR, Monorail and Nishitetsu Bus is well developed. According to the Kitakyushu Municipal Transportation Bureau, the primary transportation for Kitakyushu citizens to work or school is mainly their vehicles, accounting for 50% of the total. In

comparison, buses and railroads account for 14% and 12%, respectively (Ministry of Land, Infrastructure, Transport and Tourism, 2016). Kitakyushu has been one of the most important industrial cities and port cities in Japan. Kitakyushu Industrial Area and Kitakyushu Metropolitan Area are two significant economic zones in the Kyushu region of Japan. Kitakyushu has established shipping relations with more than 80 countries around the world. Industries are well developed, mainly in steel and chemicals.

The ambient air was sampled on the roof of Kitakyushu University's Hibino Campus (33.89°N, 130.71°E) in Kitakyushu City (Fig. 1-1), located in Kitakyushu City. Kitakyushu City, located at the eastern edge of East Asia, with a population density of more than 940,978 people/492 km^2, is one of the most urbanized cities in Japan. Its northern shore is located in the Tsushima Strait, which connects the East China Sea with the Sea of Japan. The Hibikino campus is located in a suburban area with few large stationary emission sources within ca. 4.5 km radius. A highly industrialized urban area is located ca. 15 km east of the survey site. The residential area surrounding the survey site is still being developed. There is a road (prefectural road No.11; 16,700 vehicles/day) in the vicinity (within about 800 m) of the site (Ministry of Land, Infrastructure, Transport and Tourism, 2017). The survey site is located in the Kyushu region of Japan, where there are a number of active volcanoes (Fig. 1-1). Here, it is noteworthy that all volcanoes are located in the southern area of the survey site; the Kitakyushu City government has been measuring the concentration of nitrogen oxides (NOx)—the sum of NO and NO_2 concentrations—and wind speed at the monitoring station located ca. 3 km northwest of our survey site.

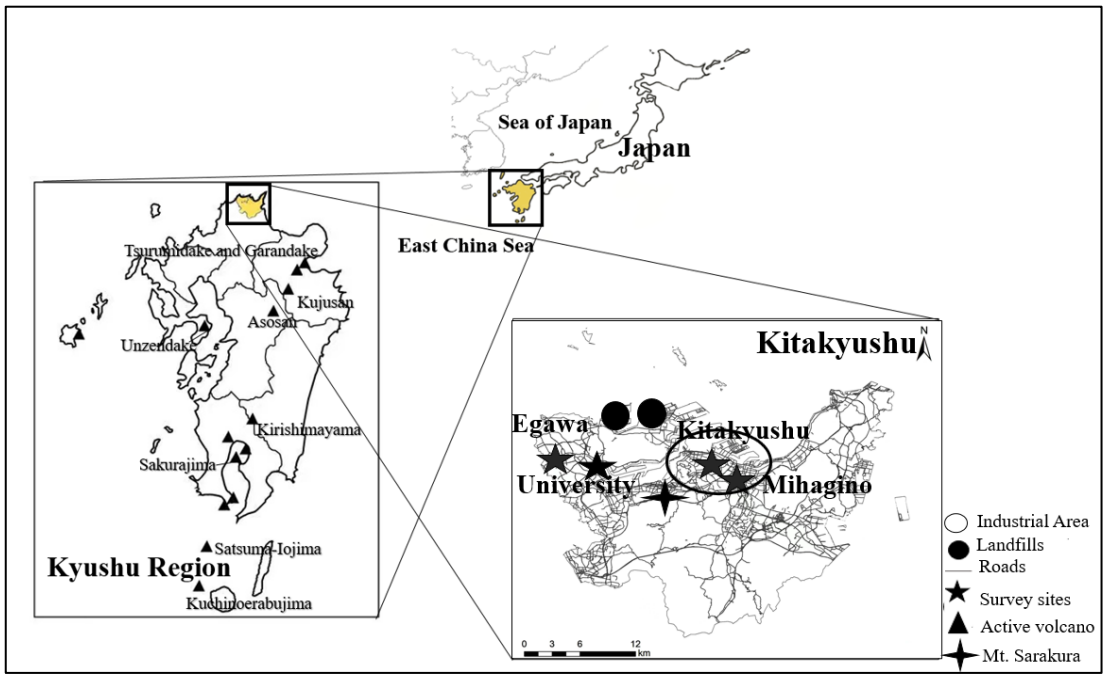

Fig.1-1. Location of survey sites and active volcanoes in Kyushu region.

Methane concentrations measured at three sites within Kitakyushu City (Egawa, Kitakyushu, and Mihagino) were statistically analyzed. The locations of the three sites are shown in Fig. 1-1. The Kitakyushu site and the Mihagino site are located in the central and downtown area of the city, having already been developed; in contrast, the Egawa site is in the suburbs of the city and is still being developed as new residential area. The city of Kitakyushu continues to measure temperature by installing a ventilated thermometer at Mt. Sarakura (summit: 622 m above sea level). Mt. Sakura is located near the central part of Kitakyushu City (Fig. 1-1). In addition, as shown in Fig. 1-1, the landfill site is located in the northwest direction of the Kitakyushu and Mihagino sites.

1.4 Research Objectives of the Present Study

Controlling the air quality is quite important to prevent health hazards/damage. There are four main components that affect air quality are emissions, transport, reactions, and deposition; and

meteorology is also one of the most important factor to control the air quality. The target area in this study forms one economic zone but complexly includes a bay as well as a mountain. This paper uses the source and dynamic behavior of HCl(g) and the measurement of atmospheric methane concentrations to understand the effects of source emissions, transboundary transport and local meteorological conditions on air quality.

This study has two specific research objectives: 1) HCl(g) is a hazardous chemical species in ambient air, so it is significant and requisite to understand and control the sources of inorganic chloride. Many previous studies on transboundary pollution have focused on non-sea salt (nss)-sulfuric (nss-SO_4^{2-}) and $PM_{2.5}$, but few studies have been done on non-sea salt chloride (nss-Cl); and presence of nss-Cl in the survey site was collected by the four-stage filter-pack method; the chapter 2, we will analyze the impact of transport on nss-Cl; 2) as we know, methane (CH_4) is chemically inert and exists in the atmosphere for a very long time (lifetime in the atmosphere exceeds 10 years). Therefore, CH_4 does not easily change its chemical form and can be used as an indicator for meteorological evaluation; we tried to evaluate the similarity/difference in the relation between the diurnal variation of the methane concentration and atmospheric conditions in an urban area different from those studied previously. The areas in the former studies were flat without large hills/mountains. In contrast, the target area in this study forms one economic zone but complexly includes a bay and a mountain. In this study, we could find the unique diurnal variation in the methane concentration and comprehensively elucidate the kinetic behavior of methane in the urban atmosphere in the central part of a big city and its suburbs.

References

Aikawa, M., Hiraki, T., Shoga, M. & Tamaki, M., 2001. Fog and precipitation chemistry at Mt. Rokko in Kobe, April 1997-March 1998. Water, Air and Soil Pollution 130, 1517-1522. https://doi.org/10.1023/A:1013945905410.

ALA, American Lung Association, 2017. www.lung.org (last access 17th Jun. 2022)

Ashrafi. K., Motlagh, M.S., Neyestani, S.E., 2017. Dust storms modeling and their impacts on air quality and radiation budget over Iran using WRF-Chem. Air Qual. Atmos. Health, 10 , pp. 1059-1076, 10.1007/s11869-017-0494-8.

Cameron, K. C., Di, H. J., Moir, J. L., 2013. Nitrogen losses from the soil/plant system: a review. Annals of applied biology, 162(2), 145-173.

Cheng, M., Zhi, G., Tang, W., Liu, S., Dang, H., Guo, Z., & Meng, F., 2017. Air pollutant emission from the underestimated households' coal consumption source in China. *Science of the Total Environment*, *580*, 641-650.

Chuang, M. T., Ooi, M. C. G., Lin, N. H., Fu, J. S., Lee, C. T., Wang, S. H., Huang, W. S., 2020. Study on the impact of three Asian industrial regions on PM $_{2.5}$ in Taiwan and the process analysis during transport. *Atmospheric Chemistry and Physics*, *20*(23), 14947-14967.

City of Kitakyushu, 2019. www.city.kitakyushu.lg.jp (last access 17th Feb. 2022).

City of Yokkaichi, 2019. www.city.yokkaichi.mie.jp (last access 7th Jun. 2022).

Conover, M. R., 2001. Resolving human-wildlife conflicts: the science of wildlife damage management. CRC press.

George, K., Ziska, L. H., Bunce, J. A., Quebedeaux, B., 2007. Elevated atmospheric CO_2 concentration and temperature across an urban–rural transect. Atmospheric Environment,

41(35), 7654-7665.

Goyal, P., Gulia, S., Goyal, S.K., 2021. Review of land use specific source contributions in PM2.5 concentration in urban areas in India. Air Qual. Atmos. Health, 14, pp. 691-704, 10.1007/s11869-020-00972-x.

Grennfelt, P., Engleryd, A., Forsius, M., Hov, Ø., Rodhe, H., Cowling, E., 2020. Acid rain and air pollution: 50 years of progress in environmental science and policy. Ambio, 49(4), 849-864.

Harrison, R. M., Van Vu, T., Jafar, H., Shi, Z., 2021. More mileage in reducing urban air pollution from road traffic. Environment International, 149, 106329.

Huang, R. J., Zhang, Y., Bozzetti, C., Ho, K. F., Cao, J. J., Han, Y., Prévôt, A. S., 2014. High secondary aerosol contribution to particulate pollution during haze events in China. Nature, 514(7521), 218-222.

Jerrett, M., Burnett, R. T., Pope III, C. A., Ito, K., Thurston, G., Krewski, D. & Thun, M., 2009. Long-term ozone exposure and mortality. *New England Journal of Medicine*, *360*(11), 1085-1095.

Kowalska, M., Ośródka, L., Klejnowski, K., Zejda, J. E., Krajny, E., & Wojtylak, M., 2009. Air quality index and its significance in environmental health risk communication. Archives of Environmental Protection, 35(1), 13-21.

Kulmala, M., Vehkamäki, H., Petäjä, T., Dal Maso, M., Lauri, A., Kerminen, V. M., McMurry, P. H., 2004. Formation and growth rates of ultrafine atmospheric particles: a review of observations. *Journal of Aerosol Science*, *35*(2), 143-176.

Lee, Y. G., Lee, H. W., Kim, M. S., Choi, C. Y., Kim, J., 2008. Characteristics of particle

formation events in the coastal region of Korea in 2005. *Atmospheric Environment*, *42*(16), 3729-3739.

Li, Y., Chiu, Y. H. & Lu, L. C., 2019. New energy development and pollution emissions in China. *International Journal of Environmental Research and Public Health*, *16*(10), 1764.

Ministry of Land, Infrastructure, Transport and Tourism, 2016. Kitakyushu City Environmental Capital Comprehensive Transportation Strategy-Kitakyushu City Regional Public Transportation Network Formation Plan. https://www.mlit.go.jp/common/001233699.pdf

Ministry of Land, Infrastructure, Transport and Tourism. 2017. http://www.mlit.go.jp/road/census/h27/index.html (last access 25th Jul. 2017).

Ministry of the Environment (MOE),2010. The English Translation of the 1996 Version (Before the MOE Was Established) Is Listed on the Website of MOE. http://www.env.go.jp/en/laws/air/air/index.html.

Murthy, B.S., Latha, R., Tiwari, A., Rathod, A., Singh, S., Beiga, G., 2020. Impact of mixing layer height on air quality in winter. J. Atmos. Sol. Terr. Phys., 197, 10.1016/j.jastp.2019.105157.

Pandey, B., Agrawal, M., Singh, S., 2014. Assessment of air pollution around coal mining area: emphasizing on spatial distributions, seasonal variations and heavy metals, using cluster and principal component analysis. Atmospheric pollution research, 5(1), 79-86.

Pant, P., & Harrison, R. M., 2013. Estimation of the contribution of road traffic emissions to particulate matter concentrations from field measurements: A review. Atmospheric environment, 77, 78-97.

Pappin, A. J., Christidis, T., Pinault, L. L., Crouse, D. L., Brook, J. R., Erickson, A., ... &

Burnett, R. T., 2019. Examining the shape of the association between low levels of fine particulate matter and mortality across three cycles of the Canadian Census Health and Environment Cohort. *Environmental health perspectives*, *127*(10), 107008.

Perlmutt, L.D., Cromar, K.R., 2019. Comparing associations of respiratory risk for the EPA Air Quality Index and health-based air quality indices. Atmospheric Environment, 202, 1-7.

Reid, C. E., Brauer, M., Johnston, F. H., Jerrett, M., Balmes, J. R., & Elliott, C. T., 2016. Critical review of health impacts of wildfire smoke exposure. Environmental health perspectives, 124(9), 1334-1343.

Sailor, D. J., & Fan, H., 2002. Modeling the diurnal variability of effective albedo for cities. Atmospheric Environment, 36(4), 713-725.

Smith, T. W. P., Jalkanen, J. P., Anderson, B. A., Corbett, J. J., Faber, J., Hanayama, S., Pandey, A., 2015. Third IMO greenhouse gas study 2014.

Srivastava, D., Xu, J., Vu, T. V., Liu, D., Li, L., Fu, P., Harrison, R. M., 2021. Insight into $PM_{2.5}$ sources by applying positive matrix factorization (PMF) at urban and rural sites of Beijing. Atmospheric Chemistry and Physics, 21(19), 14703-14724.

Strak, M., Janssen, N., Beelen, R., Schmitz, O., Vaartjes, I., Karssenberg, D., Hoek, G., 2017. Long-term exposure to particulate matter, NO_2 and the oxidative potential of particulates and diabetes prevalence in a large national health survey. Environment international, 108, 228-236.

Tian, M., Gao, J., Zhang, L., Zhang H, Feng, C., Jia, X., 2021. Effects of dust emissions from wind erosion of soil on ambient air quality. Atmos. Pollut. Res., 12 (7), 10.1016/j.apr.2021.101108

Udemba, E. N., Magazzino, C., Bekun, F. V., 2020. Modeling the nexus between pollutant emission, energy consumption, foreign direct investment, and economic growth: new insights from China. *Environmental science and pollution research*, *27*(15), 17831-17842.

Wang, Z. B., Hu, M., Sun, J. Y., Wu, Z. J., Yue, D. L., Shen, X. J., Wiedensohler, A., 2013. Characteristics of regional new particle formation in urban and regional background environments in the North China Plain. *Atmospheric Chemistry and Physics*, *13*(24), 12495-12506.

Weber, R. J., Lee, S., Chen, G., Wang, B., Kapustin, V., Moore, K., ... & Fuelberg, H. E. (2003). New particle formation in anthropogenic plumes advecting from Asia observed during TRACE-P. *Journal of Geophysical Research: Atmospheres*, *108*(D21).

WHO (World Health Organization). 2016. Global Urban Ambient Air Pollution Database, http://www.who.int/mediacentre/news/releases/2016/air-pollution-estimates/en/.

WHO (World Health Organization). 2018. 9 out of 10 people worldwide breathe polluted air, but more countries are taking action, https://www.who.int/news/item/.

WMO (World Meteorological Organization), Preventing disease through healthy environments: a global assessment of the burden of disease from environmental risks, 2012. https://www.who.int/data/gho/data/themes/public-health-and-environment.

WMO (World Meteorological Organization), WMO Air Quality and Climate Bulletin. No. 1, 2021. https://library.wmo.int/doc_num.php?explnum_id=10887.

Xu, J., Srivastava, D., Wu, X., Hou, S., Vu, T. V., Liu, D., Shi, Z., 2021. An evaluation of source apportionment of fine OC and $PM_{2.5}$ by multiple methods: APHH-Beijing campaigns as a case study. Faraday Discussions, 226, 290-313.

Yang, M., Ma, T., Sun, C., 2018. Evaluating the impact of urban traffic investment on SO_2 emissions in China cities. Energy Policy, 113, 20-27.

Yin, X., Kang, S., Rupakheti, M., de Foy, B., Li, P., Yang, J., Rupakheti, D., 2021. Influence of transboundary air pollution on air quality in southwestern China. *Geoscience Frontiers*, *12*(6), 101239.

Zhang, J., Gao, Y., Luo, K., Leung, L. R., Zhang, Y., Wang, K., Fan, J., 2018. Impacts of compound extreme weather events on ozone in the present and future. Atmospheric Chemistry and Physics, 18(13), 9861-9877.

Zhang, Q., Jiang, X., Tong, D., Davis, S. J., Zhao, H., Geng, G., Guan, D., 2017. Transboundary health impacts of transported global air pollution and international trade. *Nature*, *543*(7647), 705-709.

Zhang, Y., Yang, P., Gao, Y., Leung, R. L., Bell, M. L., 2020. Health and economic impacts of air pollution induced by weather extremes over the continental US. Environment International, 143, 105921.

Zhou, T., Hu, H., Chen, J., Bai, R., Wang, F., Wang, Y., Xu, K., 2021. Analysis on the contribution rates of point and area source emissions to wuhan SO_2, NO_2, $PM_{2.5}$ concentrations and atmospheric environmental capacity. Atmospheric Pollution Research, 12(11), 101209.

Zscheischler, J., Michalak, A. M., Schwalm, C., Mahecha, M. D., Huntzinger, D. N., Reichstein, M., Zeng, N., 2014. Impact of large-scale climate extremes on biospheric carbon fluxes: An intercomparison based on MsTMIP data. Global Biogeochemical Cycles, 28(6), 585-600.

Chapter 2 Presence and source attribution of airborne anthropogenic/non-sea-salt inorganic chloride determined by filter-pack method at eastern edge in East Asia

2.1 Introduction

Inorganic chloride in ambient air is one of the most interesting factors when considering air quality. Inorganic chloride exists in ambient air as gaseous components, typically such as hydrogen chloride (HCl(g)) as well as particulate matter such as ammonium chloride (NH_4Cl(p)) and calcium chloride ($CaCl_2$(p)) (e.g., Eldering et al., 1991; Matsumoto and Tanaka, 1996; Yao et al., 2003). These inorganic species play significant roles from the viewpoint of the acidification/nitrification of rainfall, and the load of material to our ecosystem. In East Asia, acid deposition is one of the serious environmental problems (Larssen et al., 2006; Vogt et al., 2007).

There are some potential natural and anthropogenic emission sources of inorganic chloride in ambient air and rainwater. Park et al. (2015) showed that the inorganic chloride sources in South Korea were seawater and coal burning. Davy et al. (2011) indicated that Mongolia's main sources of inorganic chloride were soil, road dust, and coal combustion. Yang et al. (2018) researched that coal combustion, residential biomass burning, and open biomass burning were the main sources of inorganic chloride in China. In comparison, Japan is geographically surrounded by oceans, which could mean that sea salt from sea water is potentially a predominant source (Aikawa et al., 2004; 2007; 2016). The inorganic chloride derived from sea water is primarily supplied as sea salt such as sodium chloride (NaCl(p)) and magnesium chloride ($MgCl_2$(p)) (Wright et al., 1988; Pakkanen et al., 2001). Aikawa et al. (2001) actually

indicated that the precipitation and cloud water collected in the western part of Japan had a similar Cl^-/Na^+ ratio to that of sea water. The chloride supplied by sea water can be categorized as a natural source. Volcanic eruption is also a potential natural emission source; in particular, Japan has some active volcanoes, making it possible that they are a dominant emission source of inorganic chloride. In contrast, inorganic chloride emissions also could be anthropogenic. One potential anthropogenic emission source would be waste incineration (Kaneyasu et al., 1999; Wey et al., 2008). In Japan, until the late 1990s, waste incinerators could potentially be a dominant source of inorganic chloride in ambient air as the chemical form of HCl(g) (Uchida et al., 1983; 1988). After the late of 1990s, thanks to countermeasures against dioxin emission, HCl(g) emissions from waste incinerators were also suppressed (Olson et al., 2000; Minoura et al., 2006); however, they still potentially emit inorganic chloride to ambient air at a certain level. however, they still potentially emit inorganic chloride to ambient air at a certain level. Coal burning is another potential anthropogenic emission source (McCulloch et al., 1999; Yao et al., 2002; Xiu et al., 2004; Liu et al., 2017).

From the viewpoint of chemical form of inorganic chloride, both gaseous and particulate forms of inorganic chloride are possible, and HCl(g) and NH_4Cl(p)/NaCl(p)/$MgCl_2$(p)/$CaCl_2$(p) etc. are dominant chemical species (Eldering et al., 1991; Matsumoto and Tanaka, 1996; Yao et al., 2003). HCl(g) would mainly result from waste incineration, coal burning, and volcanic eruption (Uchida et al., 1983; 1988; Johnson and Parnell, 1986; Mori and Notsu, 1997; McCulloch et al., 1999); in contrast, NaCl(p)/$MgCl_2$(p)/$CaCl_2$(p) of particulate species would be predominantly supplied as sea salt, and NH_4Cl(p) would come from burning coal (Pakkanen et al., 2001; Xiu et al., 2004). On the other hand, not only HCl(g) but also NH_4Cl(p) could be

produced by the chemical reactions in ambient air. As for HCl(g), the chemical reaction of $NaCl(p) + HNO_3(g) \rightarrow HCl(g) + NaNO_3(p)$ can produce HCl(g); as for $NH_4Cl(p)$, the reaction of $HCl(g) + NH_3(g) \rightleftharpoons NH_4Cl(p)$ can produce $NH_4Cl(p)$. Neither of these are the primary source of emissions but secondary means of production. Taking into account these chemical reactions in ambient air, it is impossible for us to distinguish inorganic chloride derived from sea salt from that originating from sources other than sea salt based on the chemical form.

Controlling the air quality is quite important to prevent health hazards/damage. HCl(g) is a hazardous chemical species in ambient air, so it is significant and requisite to understand and control the sources of inorganic chloride. In contrast, as shown above, it is difficult to track the sources of inorganic chloride. In this study, we tried to make the tracking on the airborne inorganic chloride clear by applying the methodology of four-stage filter-pack observation.

2.2 Experimental

2.2.1 Survey site and location

Sampling of the ambient air was carried out on the roof of a building, Hibikino Campus of The University of Kitakyushu (33.89°N, 130.71°E) (Fig. 2-1), located in Kitakyushu City. Kitakyushu City, located at the eastern edge of East Asia, with a population density of more than 961,000 people/492 km^2, is one of the most urbanized cities in Japan. Its northern shorelines are on the Tsushima Straits between the East China Sea and the Sea of Japan. The Hibikino Campus is located in the suburbs, where there are few large stationary emission sources within a 4.5 km radius. A highly industrialized downtown area is located ca. 15 km east of the survey site. The residential area surrounding the survey site is still being developed.

There is a road (prefectural road No.11; 16,700 vehicles/day) in the vicinity (within about 800 m) of the site (Ministry of Land, Infrastructure, Transport and Tourism, 2017).

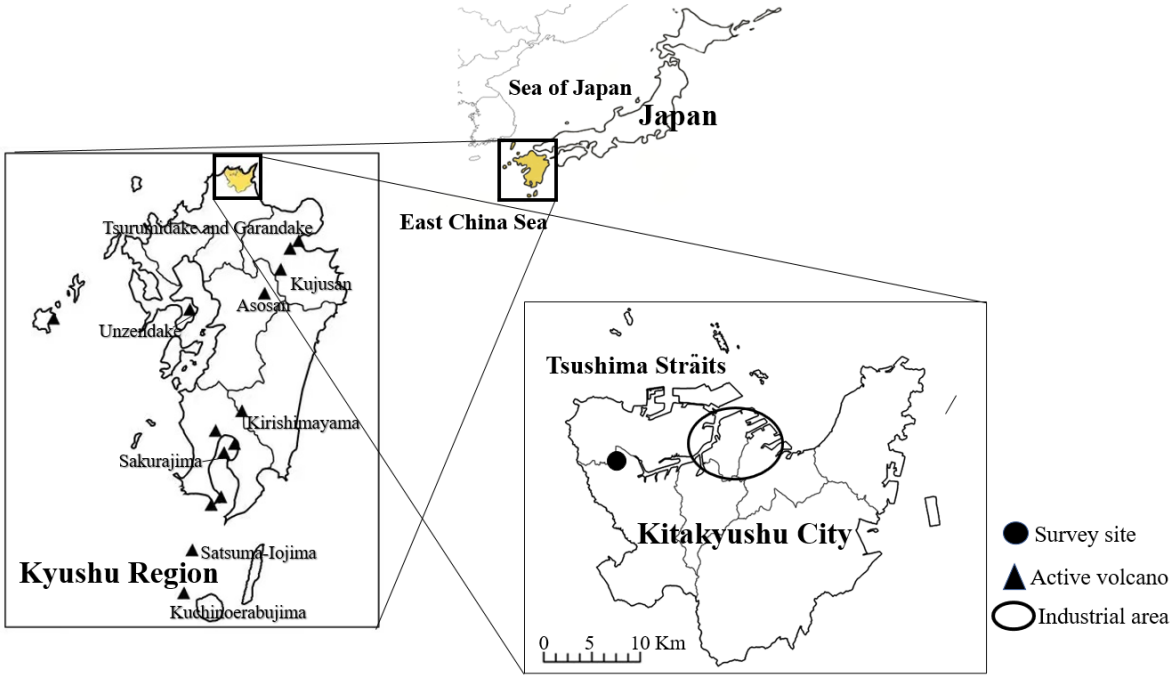

Fig.2-1 Location of survey site and active volcanoes in Kyushu region.

2.2.2 Sample collection and analysis

2.2.2.1 Method and period

Samples of the ambient air were collected year-round from December, 2016, to November, 2017, on a daily basis from 12:00 pm to 12:00 pm Japan Standard Time (JST) (24-hour sampling).

The ambient air was collected by the four-stage filter-pack method with a flow rate of 9–10 L/min; the details of the method are described in previous manuscripts (e.g., Sickles et al., 1999; Aikawa et al., 2005; Aikawa and Hiraki, 2008; 2010; Zhang et al., 2021). The employed method can simultaneously determine the concentrations of particulate matter (SO_4^{2-}, NO_3^-, Cl^-, Na^+, NH_4^+, K^+, Ca^{2+}, and Mg^{2+}) and gaseous species (SO_2, HNO_3, HCl, and NH_3), although the error

due to chemical reactions on the filter, the so-called “artifact,” cannot be definitely avoided (e.g., Matsumoto and Okita, 1998). A method of handling the artifact is described below (section 2.2.2.3).

2.2.2.2 Chemical analysis

The ion chromatograph system (Thermo Scientific™ Dionex™ Integrion, Thermo Fisher Scientific Inc., Waltham, MA, USA) used in the chemical analysis consists of a pre-column (Thermo Scientific Dionex IonPac™ AG23), a separation column (Dionex IonPac AS23), and an auto-suppressor (Thermo Scientific Dionex AERS 500 Carbonate, 4 mm) for anion analysis and a pre-column (Dionex IonPac CG16-4 μm), a separation column (Dionex IonPac CS16-4 μm), and an auto-suppressor (Thermo Scientific Dionex CERS 500, 4 mm) for cation analysis (Zhang et al., 2021).

2.2.2.3 Handling of the artifact

Cl^- in both particulate matter (Cl^-(p)) and HCl gas (HCl(g)) are susceptible to the artifact, indicating that it is difficult to determine the correct concentrations of Cl^-(p) and HCl(g) in ambient air using the four-stage filter-pack method. On the other hand, the physical quantity of chloride should be conserved as total chloride, although the artifact cannot be definitely avoided. We studied the presence and a source attribution of non-sea-salt inorganic chloride in ambient air by using this conservative quantity in the following analysis.

2.2.3 Statistical analysis

2.2.3.1 Backward trajectory analysis

In order to reveal the transport channel of air masses to our survey site, the Hybrid Single-Particle Lagrangian Integrated Trajectory (HYSPLIT) model was combined with the NCEP/GDAS meteorological data to calculate the backward trajectory, starting 15:00 UTC (0:00 JST), at heights of 1500 m above ground level at our survey site. The 72 h backward trajectory we adopted this time better reflects the characteristics of pollutant transport across regions (Wang et al., 2015). The HYSPLIT model is a professional model jointly developed by the National Oceanic and Atmospheric Center (NOAA) and the Australian Bureau of Meteorology for calculating air mass trajectories and simulating air mass dispersion and deposition (Stein et sl., 2015). The model can calculate backward air quality trajectories at different altitudes and times for a given meteorological data set (Wang et al., 2009). The categorization of wind directions in section 2.3.3.1 was carried out based on this backward trajectory. Further, a trajectory clustering method was employed to examine the pathway of air masses. In this article, all trajectory cluster analysis was based on TrajStat software, in which Ward's minimum variance method was used as a systematic clustering method. This method is widely used in backward trajectory clustering analysis (Wang et al., 2009; Zhang et al., 2020).

2.2.3.2 PSCF and CWT analyses

In the calculation method based on the backward trajectory, the potential pollution source contribution function (PSCF) algorithm is frequently used to identify the pollution source area (Ashbaugh et al., 1985). Equation (1) can be used to calculate the PSCF at the (i,j) grid cell:

$$PSCFij = \frac{m_{ij}}{n_{ij}} \quad (1)$$

Where n_{ij} is the total number of all trajectory endpoints passing through the (i, j) grid cell m_{ij} is the total number of trajectory endpoints in the same grid cell where the measured pollutant concentration exceeds the threshold value specified for that pollutant.

Further, by assigning the value of the concentration to the corresponding trajectory, the concentration-weighted trajectory (CWT) method can identify the potential source and distinguish the source intensity (Gogoi et al., 2011). The CWT is calculated as shown in equation (2).

$$C_{ij} = \frac{\sum_{l=1}^{m} C_l \tau_{ijl}}{\Sigma_{l=1}^{m} \tau_{ijl}} \quad (2)$$

Where C_{ij} is the weighted average concentration of the *(i,j)*th grid cell, i is the index of the trajectory m is the total number of trajectories, C_l is the pollutant concentration corresponding to the trajectory l when it passes through the network cell *(i,j)*, τ_{ijl} is the residence time of the trajectory l in the grid cell *(i,j)*. TrajStat software was employed for PSCF and CWT analyses (Wang et al., 2009). The specific flow chart and grid distribution are shown in Fig. 2-2.

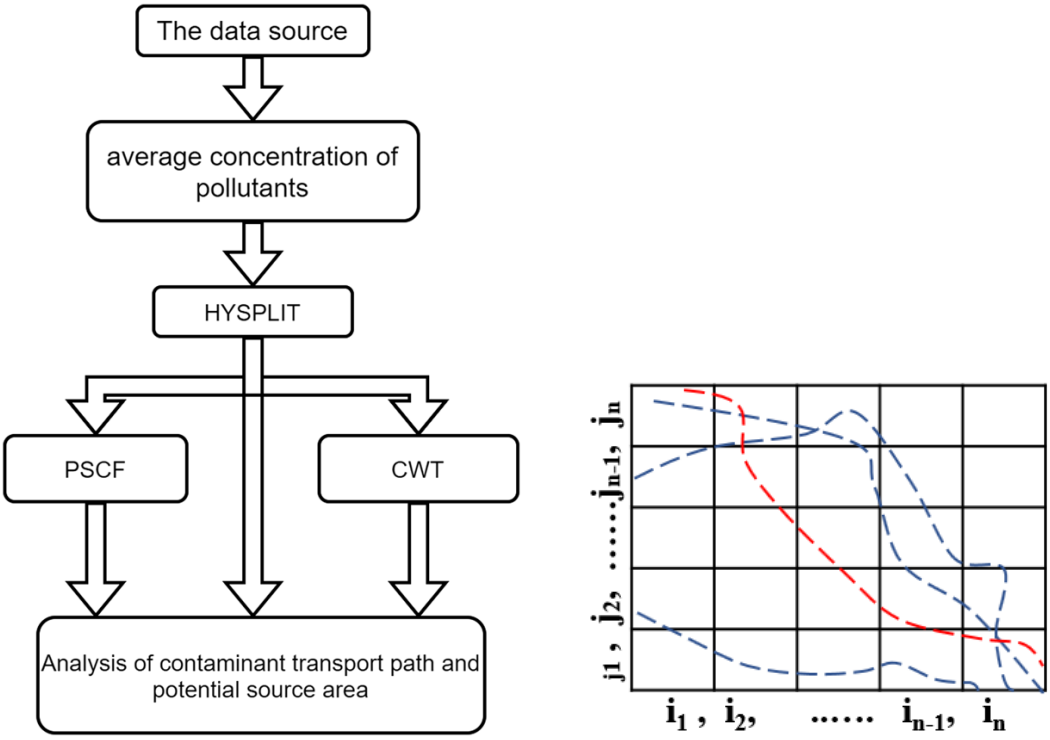

Fig. 2-2 The flowchart of main research methods of HYSPLIT, PSCF and CWT models (Ma et al., 2021) and the gird cell distribution map, including trajectories (the red line was a polluted trajectory, blue line were trajectories concentration lower than the threshold value).

2.2.4 Calculation of nss-chloride

The concentrations of non-sea-salt (nss)-chloride (nss-Cl) were calculated based on the Na^+ concentration, assuming that all Na^+ is derived from sea salt. In this study, we mainly focus on the source of nss-Cl. For all particulate matter and gaseous species measured in the four-stage filter-pack method, we only used the concentration of Cl^-(p), HCl(g), and Na^+(p).

2.2.5 Seasonal classification

In statistical analyses, we adopted seasonal classifications—winter (December, January, February), spring (March, April, May), summer (June, July, August), and autumn (September, October, November).

2.2.6 Analyses of meteorological dependence

The Kitakyushu City government has been measuring the concentration of nitrogen oxides (NOx)—the sum of NO and NO_2 concentrations—and wind speed at the monitoring station located ca. 3 km northwest of our survey site. We obtained these data on NOx concentration and wind speed on the open website (National Institute for Environmental Studies, 2020) and used them to analyze the relationship with wind (section 2.3.3.3).

2.3 Results and discussion

2.3.1 Variations in concentrations of particles and gas

2.3.1.1 Cl^-(p) and HCl(g)

Fig. 2-3(a) and (b) shows the temporal change of the Cl^-(p) and HCl(g) concentrations, respectively, on a daily basis determined by the four-stage filter-pack method. A statistically significant ($p<0.05$) seasonal variation was observed in both Cl^-(p) and HCl(g) concentrations; winter (72.4 $nmol \cdot m^{-3}$) ≈ autumn (71.2) > spring (42.9) > summer (26.1) in Cl^-(p) and spring (36.9) ≈ summer (36.7) > winter (27.1) > autumn (21.2) in HCl(g), as summarized in Table 1. Whereas the Cl^-(p) and HCl(g) concentrations are affected reciprocally by the artifact, total chloride (T-Cl)—the sum of Cl^-(p) and HCl(g) concentrations—is conserved (section 2.2.2.3). The T-Cl concentration showed seasonal variations similar to those of the Cl^-(p) concentration; higher in winter and lower in summer (Table 2-1). Whereas the Cl^-(p) and HCl(g) concentrations are affected reciprocally by the artifact, total chloride (T-Cl)—the sum of Cl^-(p) and HCl(g) concentrations—is conserved (section 2.2.2.3). The T-Cl concentration showed seasonal variations similar to those of the Cl^-(p) concentration; higher in winter and lower in

summer (Table 2-1). This is because the inorganic chloride in ambient air is mainly attributable to sea salt derived from sea water, as Aikawa et al. (2016) actually demonstrated that the ambient chloride was attributable to sea salt. This attribution will be analyzed and discussed in more detail in the next section.

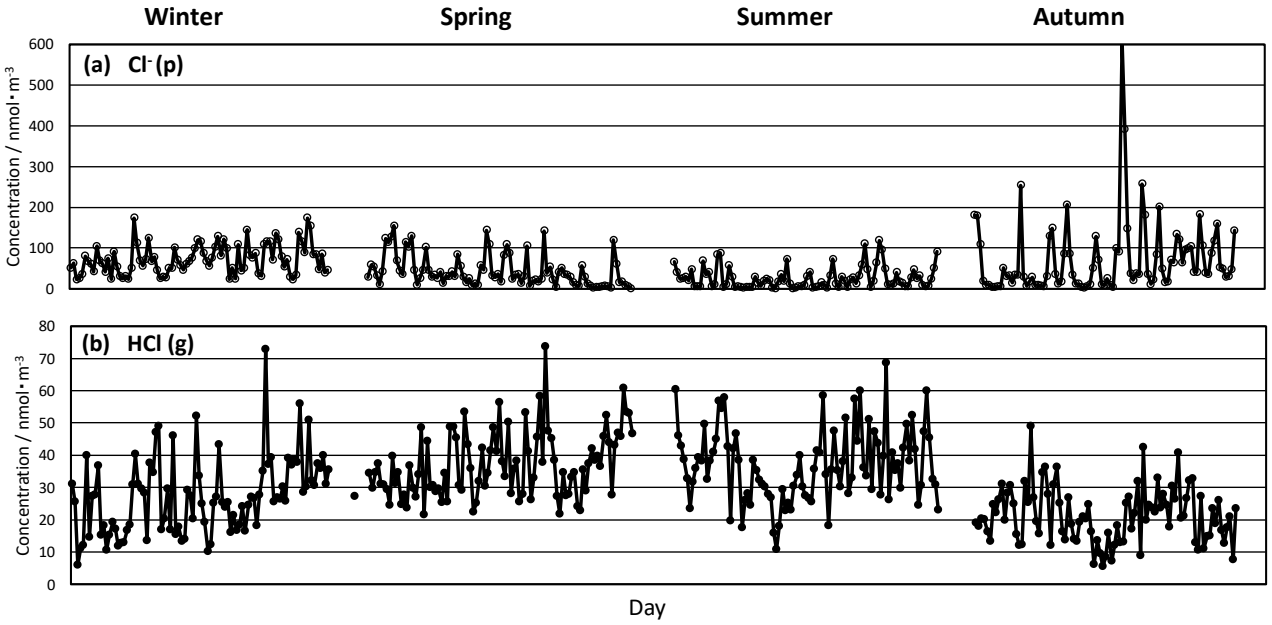

Fig. 2-3 Temporal variations of Cl^-(p) (a) and HCl(g) concentrations (b).

Table 2-1 Seasonal mean concentrations (nmol・m^{-3}) and their statistical difference on chloride species.

	Cl^-(p)	statistical difference*	HCl(g)	statistical difference*	T-Cl	statistical difference*	nss-Cl	statistical difference*
Spring	**42.9**	**b**	**36.9**	**a**	**79.7**	**b**	**13.3**	**a**
Summer	**26.1**	**c**	**36.7**	**a**	**62.8**	**c**	**9.4**	**b**
Autumn	**71.2**	**a**	**21.2**	**c**	**92.3**	**ab**	**4.4**	**c**
Winter	**72.4**	**a**	**27.1**	**b**	**99.5**	**a**	**9.1**	**b**

*Statistical difference is based on $p<0.05$

2.3.1.2 Scatter plot of T-Cl to Na^+(p) and nss-chloride

Total chloride is conserved, even though both Cl^-(p) and HCl(g) concentrations are affected

reciprocally by the artifact; therefore, we use T-Cl (= Cl^-(p) + HCl(g)) here to consider the relationship between chloride species and sodium. Fig. 2-4 shows the scatter plot of T-Cl to Na^+(p) by the unit of nmol·m^{-3} for each season. The molar ratio of Cl^- for Na^+ in seawater is 1.17 (Wilson, 1975). Although seasonal variation can be seen, the slopes in Fig. 2-4 were close to 1.17 in all seasons. Assuming that all sodium is derived only from seawater, inorganic chloride in the ambient air could also be involved in sea water.

Meanwhile, interestingly, the approximate curve, except in autumn, had certain intercepts: 12.4 nmol·m^{-3} for winter, 21.5 for spring, 17.5 for summer, and -2.9 for autumn. As for autumn, the concentration was evenly distributed over a wide range, from the high to low concentrations. This mainly would be due to the typhoon events Japan experiences every year. As a consequence, both chloride and sodium concentrations were strongly influenced by seawater, presumably resulting in the large coefficient of determination (0.99), the slope (1.22) close to 1.17, and the intercept (-2.9 nmol·m^{-3}) close to zero. In contrast, certain intercepts were observed in the other three seasons. These intercepts suggest that a certain chloride existed in the ambient air even though no sodium is supplied from seawater. We can regard this chloride given by the intercept as non-sea-salt chloride, as shown by the next equation.

Non-sea-salt (nss) chloride (nss-Cl) = Total chloride (T-Cl) – $Na^+_{(observed)} \times (Cl^-/Na^+)_{seawater}$, where Total chloride (T-Cl) = the sum of Cl^-(p) and HCl(g) concentrations determined by the observation, $Na^+_{(observed)}$ = Na^+ concentrations determined by observation, and $(Cl^-/Na^+)_{seawater}$ = 1.17.

Further, this nss-Cl can be considered to be released from anthropogenic emission sources and/or chloride released from natural emission sources, such as a volcanic eruption.

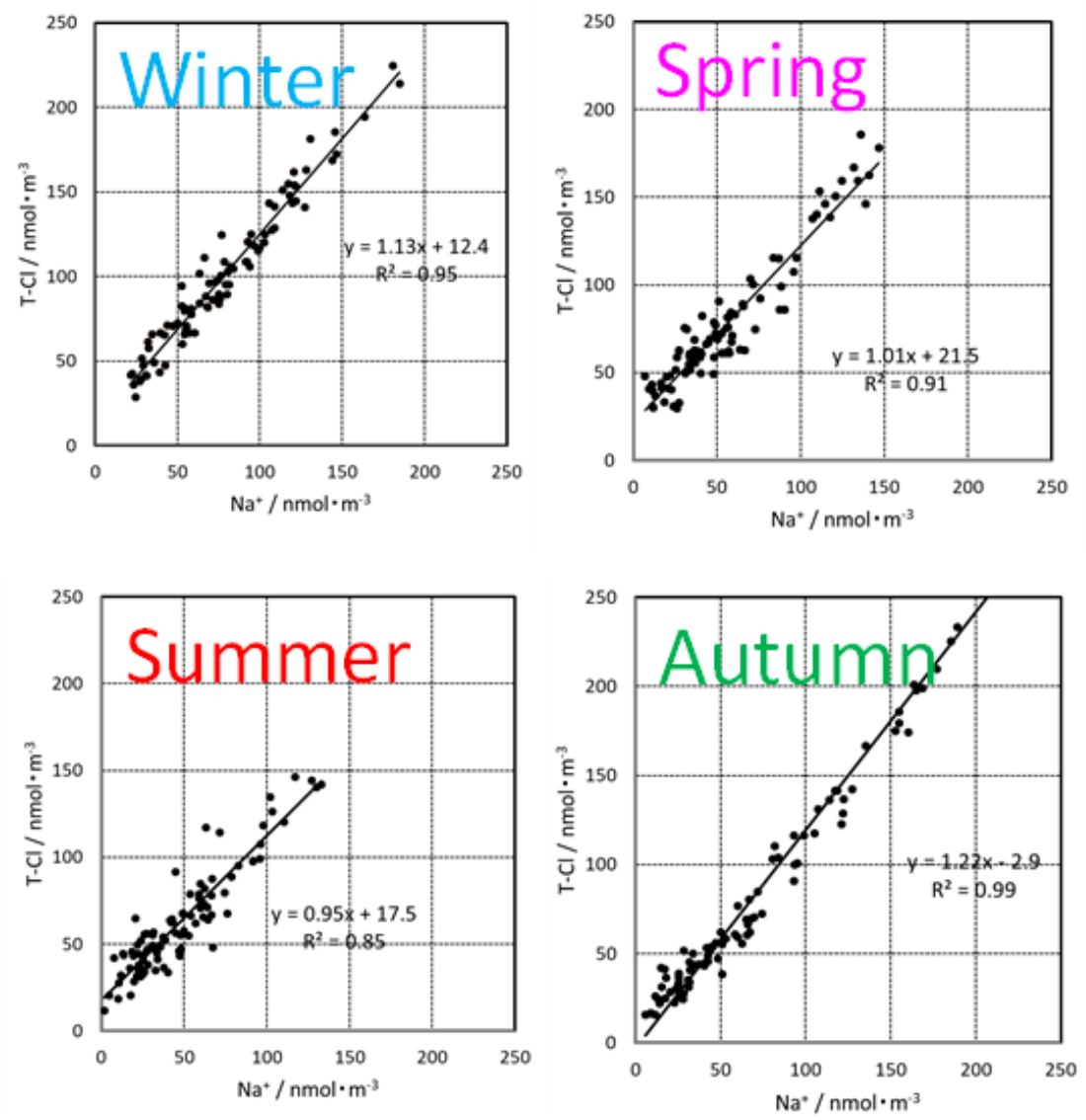

Fig. 2-4. Scatter plot of T-Cl concentration for Na^+(p) concentration in each season.

2.3.2 Variation in the concentration of nss-Cl and the definition of high nss-Cl concentrations

2.3.2.1 Temporal and seasonal variation of nss-Cl concentrations

Fig. 2-5(a) shows temporal variations of nss-$Cl_{(raw)}$ concentrations. In this nss-$Cl_{(raw)}$ concentration, negative values are plotted without changing. The calculated nss-Cl concentration based on the above equation has a negative value—certainly due to its inherently

low concentration, likely due to some assumptions in its calculation process, and slightly due to some errors in the observation and chemical analyses. However, these negative values have no physical/chemical meaning; therefore, it is appropriate to regard these negative values as zero. Fig. 2-5(b) shows the temporal variation of nss-Cl concentrations after replacing the negative values with zero. Temporal variations were observed in each season.

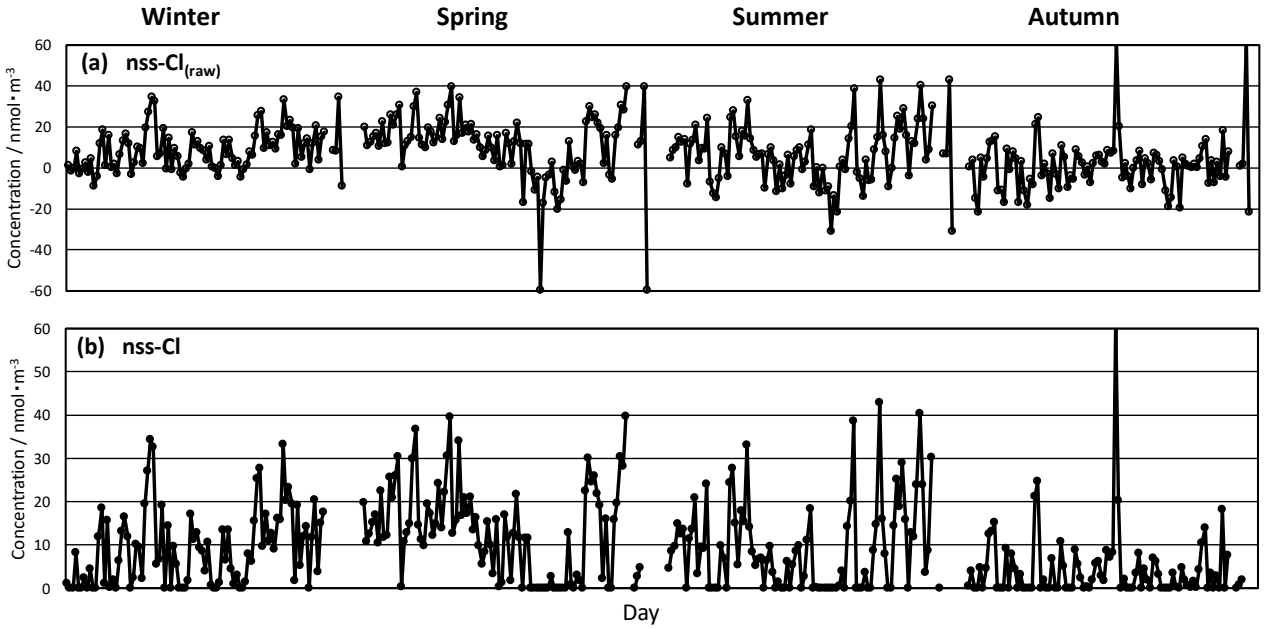

Fig. 2-5. Temporal variations of nss-$Cl_{(raw)}$ (a) and nss-Cl concentrations (b).

The seasonal mean of the nss-Cl concentration and its statistical differences are summarized in Table 2-1. The nss-Cl concentration was higher in spring and lower in autumn. This seasonal variation was similar to that of HCl(g), although the nss-Cl concentration in summer was relevant to that in the winter while the HCl(g) concentration in summer was relevant to that in spring. Cl^-(p) and HCl(g) are reciprocally susceptible to the artifact (2.2.2.1 and 2.2.2.3). The dissociation of NH_4Cl(p) is more sensitive to the change in ambient temperature than that of NH_4NO_3 (Kaneyasu et al., 1999); this is probably responsible for the relevant HCl(g) concentration in summer as compared to that in spring.

2.3.2.2 Frequency distribution of nss-Cl concentration

Table 2-2 shows the frequency statistics of different concentrations of nss-Cl. The original negative concentration replaced by zero accounted for the largest frequency (ca. 28%), and the frequency monotonically decreased, combined with an increasing nss-Cl concentration. Kaneyasu et al. (1999) carried out the extensive field measurements and discussed the chemical form and sources of extremely high chloride in winter aerosol pollution near Metropolitan Tokyo. We also studied source attribution of the high concentrations of nss-Cl. For this purpose, we defined high concentration nss-Cl as being higher than 20 nmol·m^{-3}. This definition is based on the proportion of days whose concentration was higher than 20 nmol·m^{-3}, which was ca. 14%—close to 90 percentile. As a consequence, 50 days were categorized as high nss-Cl– concentration days. Source attributions were studied for these 50 days by means of statistical analyses and their correlation with the meteorological parameters.

Table 2-2 Frequency statistics of different concentrations of nss-Cl.

nss-Cl mean concentration /nmol·m^{-3}	Number of days	Frequency / %
nss-Cl ≤0	102	27.9
0 < nss-Cl ≤ 5.0	66	18.1
5.0 < nss-Cl ≤ 10.0	55	15.1
10.0 < nss-Cl ≤ 15.0	54	14.8
15.0 < nss-Cl ≤ 20.0	38	10.4
20.0 < nss-Cl ≤ 25.0	22	6.0
25.0 < nss-Cl ≤ 30.0	12	3.3
30.0 < nss-Cl ≤ 35.0	9	2.5
nss-Cl > 35.0	7	2.0

2.3.3 Source attribution of high nss-Cl concentration

2.3.3.1 Backward trajectory analysis

The backward trajectories were calculated based on the methodology mentioned in 2.2.3.1. Sampling was carried out throughout one year, resulting in the calculation of 365 backward

trajectories. These 365 backward trajectories were categorized by the direction by which the wind arrived at the survey site: (1) north, (2) south, and (3) others. North, for instance, means that the wind arrived at the survey site without going to the southern areas before arriving at the survey site. Others means that the wind passed through both the northern and the southern areas before arriving at the survey site.

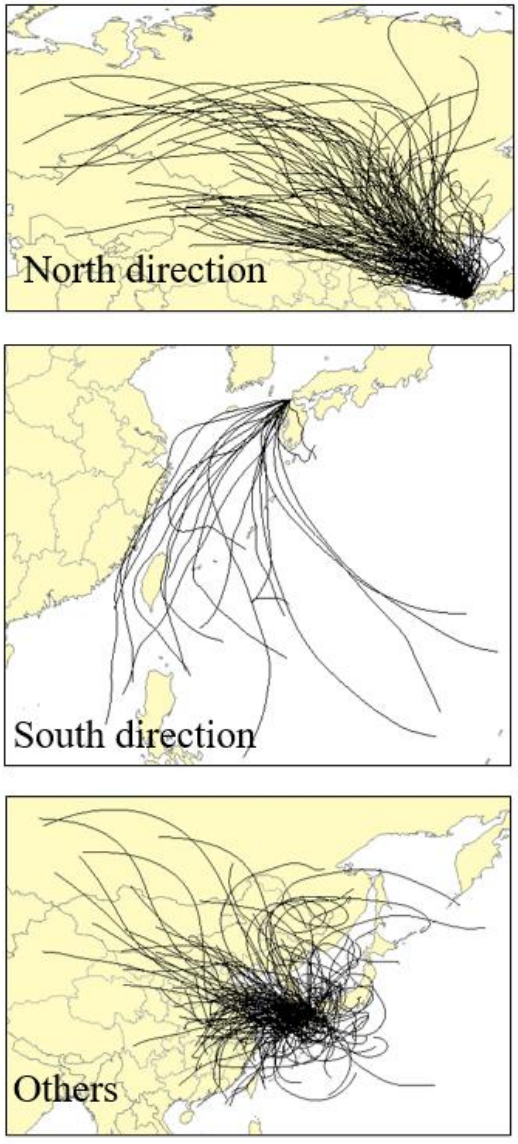

Fig. 2-6. Backward trajectories categorized in three categories.

Fig. 2-6 shows the backward trajectories categorized into the three categories for the total days of the survey. There were 176, 23, and 166 days, respectively, with north, south, and other winds,

corresponding to ca. 50, 5, and 45 percents, respectively. On the other hand, Fig. 2-7 shows the backward trajectories of the high nss-Cl–concentration days, together with the top five highest nss-Cl–concentration days. There were 29, 1, and 20 days, respectively, with north, south, and other winds, corresponding to ca. 58, 2, and 40 percents, respectively. Both the number and the rate of the days categorized as south in the high nss-Cl concentration were smaller than those of the year-round data. The survey site is located in the Kyushu region in Japan, where some active volcanoes are located (Fig. 2-1). Here, it is noteworthy that all volcanoes are located in the southern area of the survey site; therefore, if the influence from the volcano appears on the survey site, it is assumed that the southern wind would provide the higher nss-Cl concentration for the survey site. However, the actual observation data was opposite that expected, strongly suggesting that the volcano's influence on the nss-Cl concentration at the survey site was not so severe.

Furthermore, mean nss-Cl concentrations in each category year round were 9.9 $nmol \cdot m^{-3}$ for north, 6.6 for south, and 8.5 for others, indicating that the northern wind apparently provides a higher nss-Cl concentration, even from the viewpoint of the year-round data.

The upper right corner of Fig. 2-7 shows the backward trajectory for the top five highest nss-Cl–concentration days—Oct. 22, Aug. 13, Aug. 27, May 31, and Mar. 31—and the corresponding nss-Cl concentrations were 61.7, 42.8, 40.3, 39.7, and 39.5 $nmol \cdot m^{-3}$, respectively. Zhang et al. (2021) demonstrated that the air masses arriving at the survey site on May 31, Aug. 13, and Aug. 27 were strongly influenced by industrial combustion and ship emissions. The gaseous pollutants in the exhaust gas from marine vessels include HCl(g) (Bence et al., 2020), suggesting that high nss-Cl–concentration days were strongly influenced

by anthropogenic emissions from marine vessel. The backward trajectories on Oct. 22 and Mar. 31 originated from the continent and arrived at the survey site after passing over the Sea of Japan. The air mass on Oct. 22 passed through Changchun on Oct. 19, and Changchun experienced a severe air pollution incident on that day; the air quality index (AQI) was 186 (Ministry of Ecology and Environment of China, 2020). A similar situation was observed on Mar. 31; an air mass passed through Qiqihar on Mar. 29 and Changchun on Mar. 30; these cities experienced air pollution events on the corresponding days: the AQIs were 82 and 120, respectively. The air masses passing through these polluted cities presumably provided the extremely high anthropogenic nss-Cl concentration at our survey site.

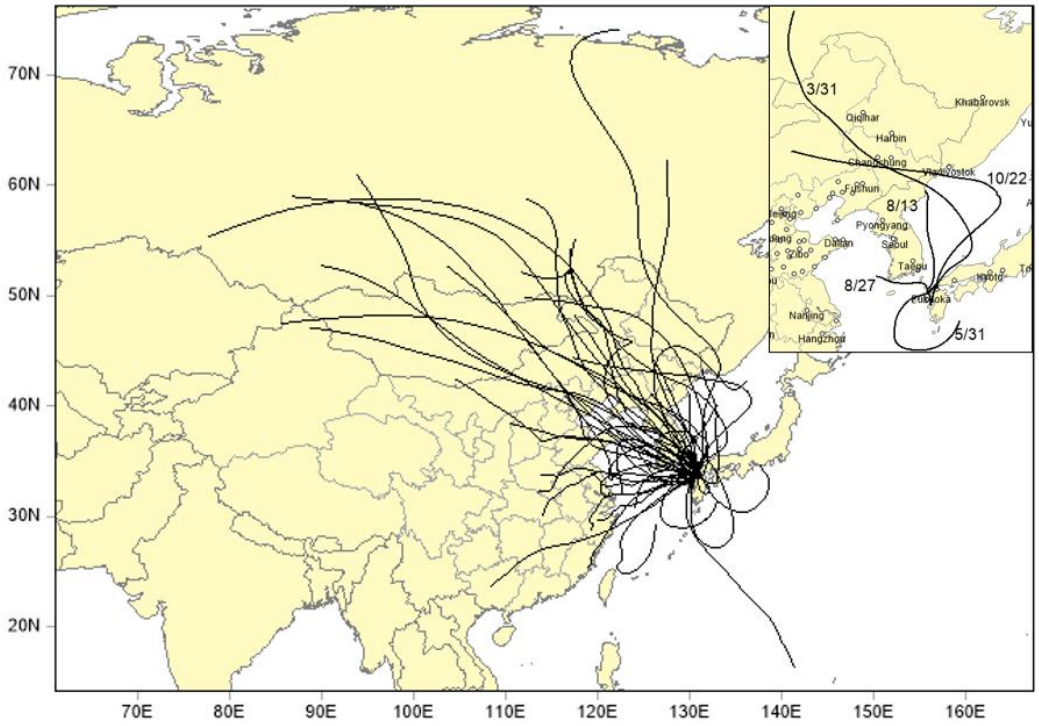

Fig. 2-7. Backward trajectories in the high nss-Cl concentration days together with the top five highest nss-Cl concentration days.

2.3.3.2 PSCF and CWT analyses

The PSCF and CWT methods were used to discuss the potential sources and contributions of anthropogenic/nss-Cl at the survey site. The results are shown in Fig. 2-8. As shown in Fig. 2-8(a), the large value areas of PSCF (PSCF value >0.7) were mainly concentrated in four parts. The first part was long-distance pollutants northwest of the survey site, mainly in Russia and Mongolia. In 2017, there were 9,537 forest fires in Russia (Podolskaia et al., 2020), in which a great quantity of biomass was burned; the combustion of biomass produces hydrogen chloride (Ren et al., 2017; Zhang et al., 2020), indicating that the nss-Cl anthropogenically generated would arrive at the survey site by the transported air masses. Mongolia has serious and frequent air pollution (Ganbat et al., 2020; Nirmalkar et al., 2020); in a report by Sophie (2019), most of the air pollution that occurred in Mongolia in 2017 was caused by the use of coal for heating. Under the influence of monsoons, a large amount of anthropogenic nss-Cl would be transported to the survey site.

The second part was in the north of the survey site, consisting of two areas: (1) the long-distance potential source area, Russia; and (2) northeast China and the Sea of Japan. Finding the long-distance potential source area in Russia might be beyond the limitations of the PSCF method. When air masses pass over distant grid cells, those grid cells sometimes include only a few trajectory points. In such a situation, those grid cells sometimes have extreme PSCF values with a high uncertainty (Dimitriou and Kassomenos, 2016). Many air masses originated in northeastern China and arrived at the survey site after passing over the Sea of Japan, and these air masses were similar to those on Oct. 22 and Mar. 31, as mentioned in 2.3.3.1 and Fig. 2-7. The average rate of occurrence frequency of air pollution events based on the AQI (PM2.5) for

Northeast China in 2017 was 16% (12%) (Fan et al., 2020), showing that northeastern China would be an important potential source area for anthropogenic nss-Cl.

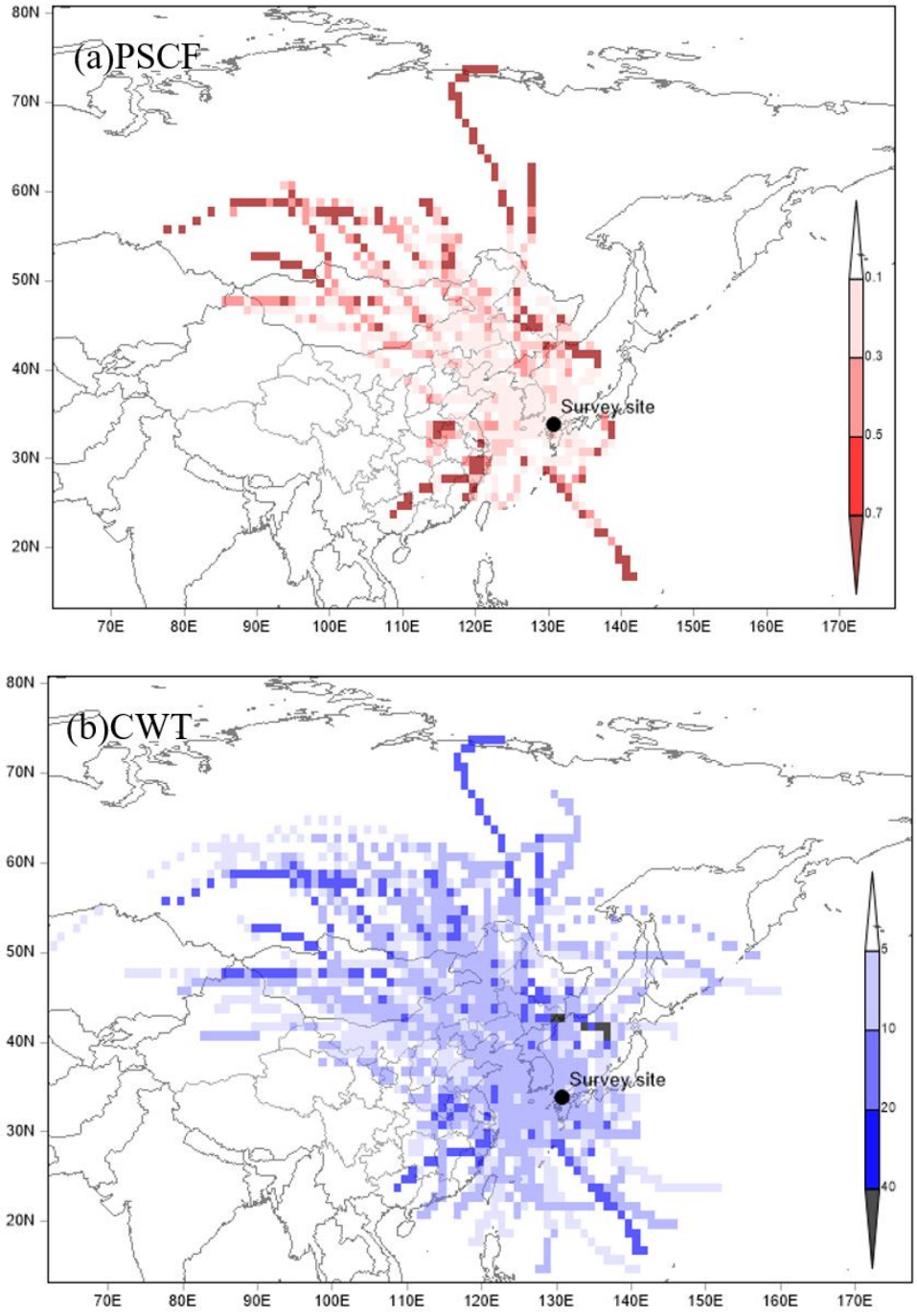

Fig. 2-8. Potential source contribution function for anthropogenic/nss-Cl (a) and concentration weighted trajectory for anthropogenic/nss-Cl (b) at survey site.

The third part was in the southwest, mainly in the south of China, including Jiangsu, Zhejiang, Fujian, and Jiangxi. All of these Chinese cities are industrial areas with large populations. Previous studies showed that these cities produced a large amount of anthropogenic nss-Cl through industrial production and coal burning (Liu et al., 2017; Yang et al., 2018). This anthropogenic nss-Cl would be also transported to the survey site through transboundary airflow.

The fourth part is located in south of the survey site, mainly in the marine area. The potential source of nss-Cl in the marine area is close to Japan, and the source for the event on May 31 was emissions from marine vessels (Zhang et al., 2021). On the other hand, we showed that there were few trajectories from the south (ca. 5%) (section 3.3.1), and these grid cells included only a few trajectory points, leading to extreme PSCF values in these specific cells.

The results of the CWT plots (CWT > 20 nmol/m^3) shown in Fig. 2-8(b) also showed that the main contribution areas of anthropogenic/nss-Cl to the survey sites were the same areas as shown by PSCF analysis. These results indicate that most areas contributing to the anthropogenic/nss-Cl concentrations at the survey site were in the northwest, north, and southwest.

2.3.3.3 Relationship with wind speed

Kaneyasu et al. (1999) discussed HCl(g) from waste incinerator as the precursor of Cl^- in aerosols, and the emission from the incineration of domestic and industrial waste near Metropolitan Tokyo was estimated to be the source. Kitakyushu City is one of the most urbanized cities in Japan, and its population density is more than 961,000 people/492 km^2;

therefore, the influence of domestic emission sources should be evaluated. In this study, we evaluated domestic influences based on the relationship of the concentration and the wind speed.

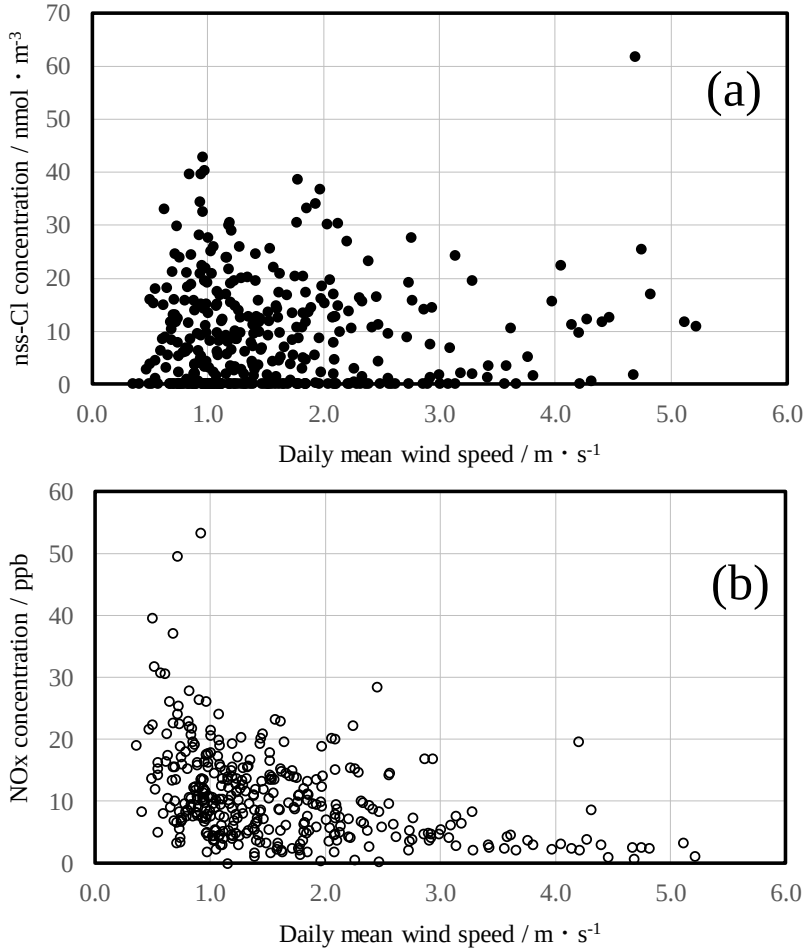

Fig. 2-9. Relationship of the nss-Cl (a) and NOx (b) concentrations with daily mean wind speed.

Fig. 2-9(a) and (b) shows, respectively, the relationship of the nss-Cl and NOx concentrations with the daily mean wind speed. The NOx concentration was used here as a representative parameter to present domestic/local emissions. No clear relationship between the nss-Cl concentration on the wind speed (the Pearson correlation coefficient: -0.09 ($p>0.05$)), i.e. no dependence of the nss-Cl concentration and the wind speed, was observed (Fig. 2-9(a)) while the dependence of the NOx concentration on the wind speed was shown (Fig 2-9(b)). In addition,

zero nss-Cl concentrations were frequently observed, even under weak wind speeds, most likely suggesting that domestic emissions were not the parameter controlling the nss-Cl concentration around the survey area in the present.

2.4 Conclusions

The anthropogenic/non-sea-salt (nss) inorganic chloride in ambient air was evaluated from the viewpoint of its presence and source attribution by applying the four-stage filter-pack method. Observations were carried out for one year by sampling (both particulate matter and gaseous species) on a daily (24-hour) basis. The anthropogenic/nss inorganic chloride was detected on 263 days (ca. 72% of the days in one year), and concentrations higher than 20 nmol·m^{-3} were observed on 50 days (ca. 14% of the total sampling days). The source attribution was discussed, taking into account possible sources of in-country volcanic eruption, municipal waste incineration, domestic coal burning, and transboundary transportation. Concentrations of inorganic chloride higher than 20 nmol·m^{-3} were predominantly observed with a northern wind direction, while high concentrations were infrequent when there was a southern wind direction, strongly suggesting that the in-country volcanic eruption had little influence on the high concentration of nss-inorganic chloride. Wind speed had no relationship with concentrations higher than 20 nmol·m^{-3}, indicating that neither municipal waste incineration nor domestic coal burning had much impact on the high concentration. The statistical analyses of the backward trajectory indicated that the transboundary transportation from the area of the northeast and south of China, Mongolia, Russia, and the Sea of Japan contributed greatly to the high concentration of the anthropogenic/nss-inorganic chloride along the eastern edge in East Asia.

References

Aikawa, M. & Hiraki, T., 2008. Methodology of analysis associating survey results by the filter-pack method with those of precipitation - Acid-base balance on acid-related and alkali-related chemical species in urban ambient air and its influence on the acidification of precipitation. Journal of Atmospheric Chemistry, 61, 21-29. https://doi.org/10.1007/s10874-009-9122-9.

Aikawa, M. & Hiraki, T., 2010. Difference in the Use of a Quartz Filter and a PTFE Filter as First-Stage Filter in the Four-Stage Filter-Pack Method. Water, Air, and Soil Pollution, 213, 331-339. https://doi.org/10.1007/s11270-010-0388-y.

Aikawa, M., Hiraki, T. & Tamaki, M., 2005. Characteristics in concentration of chemical species in ambient air based on three-year monitoring by filter pack method. Water, Air and Soil Pollution, 161, 335 – 352. https://doi.org/10.1007/s11270-005-4774-9.

Aikawa, M., Hiraki, T., Shoga, M. & Tamaki, M., 2001. Fog and precipitation chemistry at Mt. Rokko in Kobe, April 1997-March 1998. Water, Air and Soil Pollution 130, 1517-1522. https://doi.org/10.1023/A:1013945905410.

Aikawa, M., Hiraki, T., Shoga, M. & Tamaki, M., 2004. Spatial variations and trends in acid deposition in Japan within a 100 km x 100 km region from 1986 to 1999. Water, Air and Soil Pollution 157, 225-244. https://doi.org/10.1023/B:WATE.0000038895.44587.94.

Aikawa, M., Morino, Y., Kajino, M., Hiraki, T., Horie, Y., Nakatsubo, R., Matsumura, C. & Mukai, H., 2016. Candidates to provide a specific concentration difference for ambient sulfur and nitrogen compounds near the coastal and roadside sites of Japan. Water, Air, and Soil Pollution 227: 353. https://doi.org/10.1007/s11270-016-3069-7.

Aikawa, M., Suzuki, M., Hiraki, T., Tamaki, M., Kondo, A., Mukai, H. & Murano, K., 2007. Intensive Field Survey of Aerosol and Gas Concentrations with 6-h Interval Sampling in Winter in Japan. Water, Air and Soil Pollution 182, 91-105. https://doi.org/10.1007/s11270-006-9324-6.

Ashbaugh, L.L., Malm, W.C. & Sadeh, W.Z., 1985. A residence time probability analysis of sulfur concentrations at Grand Canyon National Park. Atmospheric Environment, 19(8), 1263-1270. https://doi.org/10.1016/0004-6981(85)90256-2.

Bencs, L., Horemans, B., Buczyńska, A.J., Deutsch, F., Degraeuwe, B., Poppel, M.V. & Grieken, R.V. (2020). Seasonality of ship emission related atmospheric pollution over coastal and open waters of the North Sea. Atmospheric Environment: X, 7: 100077. https://doi.org/10.1016/j.aeaoa.2020.100077.

Davy, P.K., Gunchin, G., Markwitz, A., Trompetter, W.J., Barry, B.J., Shagjjamba, D. & Lodoysamba, S., 2011. Air particulate matter pollution in Ulaanbaatar, Mongolia: determination of composition, source contributions and source locations. Atmospheric Pollution Research, 2(2), 126-137. https://doi.org/10.5094/APR.2011.017.

Dimitriou, K. & Kassomenos, P., 2016. Combining AOT, Angstrom Exponent and PM concentration data, with PSCF model, to distinguish fine and coarse aerosol intrusions in Southern France. Atmospheric Research, 15, 74-82. https://doi.org/10.1016/j.atmosres.2016.01.002.

Eldering, A., Solomon, P.A., Salmon, L.G., Fall, T. & Cass, G.R., 1991. Hydrochloric acid: a regional perspective on concentrations and formation in the atmosphere of Southern California. Atmospheric Environment, 25A, pp. 2091-2102. https://doi.org/10.1016/0960-

1686(91)90086-M.

Fan, H., Zhao, C.F. & Yang, Y.K. (2020). A comprehensive analysis of the spatio-temporal variation of urban air pollution in China during 2014–2018. Atmospheric Environment, 220: 117066. https://doi.org/10.1016/j.atmosenv.2019.117066.

Ganbat, G., Soyol-Erdene, T.O. & Jadamba, B., 2020. Recent Improvement in Particulate Matter (PM) Pollution in Ulaanbaatar, Mongolia. Aerosol and Air Quality Research, 20: 2280–2288. https://doi.org/10.4209/aaqr.2020.04.0170.

Gogoi, M.M., Pathak, B., Moorthy, K.K., Bhuyan, P.K., Babu, S.S., Bhuyan, K. & Kalita, G., 2011. Multi-year investigations of near surface and columnar aerosols over Dibrugarh, northeastern location of India: Heterogeneity in source impacts. Atmospheric Environment, 45(9), 1714-1724. https://doi.org/10.1016/j.atmosenv.2010.12.056.

Johnson, N. & Parnel JR, R.A., 1986. Composition, distribution and neutralization of "acid rain" derived from Masaya volcano, Nicaragua. Tellus B: Chemical and Physical Meteorology, 38,106-117. https://doi.org/10.3402/tellusb.v38i2.15086.

Kaneyasu, N., Yoshikado, H., Mizuno, T., Sakamoto, K & Soufuku, M., 1999. Chemical forms and sources of extremely high nitrate and chloride in winter aerosol pollution in the Kanto Plain of Japan. Atmospheric Environment, 33, 1745-1756. https://doi.org/10.1016/S1352-2310(98)00396-3.

Larssen, T., Lydersen, E., Tang, D., He, Y., Gao, J., Liu, H. & Luo, J., 2006. Acid rain in China. https://pubs.acs.org/doi/pdf/10.1021/es0626133.

Liu, B.S., Wu, J.H., Zhang, J.Y., Wang, L., Yang, J.M., Liang, D.N., Dai, Q.L., Bi, X.H., Feng, Y.C., Zhang, Y.F. & Zhang, Q.X., 2017. Characterization and source apportionment of

PM2.5 based on error estimation from EPA PMF 5.0 model at a medium city in China. Environmental Pollution, 222:10-22. https://doi.org/10.1016/j.envpol.2017.01.005.

Ma, Y., Liu, Q., Bian, Y., Feng, L., Zhao, D., Wang, S., ... & Xu, Z., 2021. Analysis of transport path and source distribution of winter air pollution in Shenyang. Open Geosciences, 13(1), 1105-1117.

Matsumoto, K. & Tanaka, H., 1996. Formation and dissociation of atmospheric particulate nitrate and chloride: an approach based on phase equilibrium. Atmospheric Environment, 30(4),pp, 639-648. https://doi.org/10.1016/1352-2310(95)00290-1.

Matsumoto, M. & Okita, T., 1998. Long term measurements of atmospheric gaseous and aerosol species using an annular denuder system in Nara, Japan. Atmospheric Environment, 32, 1419-1425. https://doi.org/10.1016/S1352-2310(97)00270-7.

McCulloch, A., Aucott, M.L. & Benkovitz, C.M., 1999. Global emissions of hydrogen chloride and chloromethane from coal combustion, incineration and industrial activities: Reactive chlorine emissions inventory. Journal of Geophysical Research: Atmospheres, 104: 8391-8403. https://doi.org/10.1029/1999JD900025.

Ministry of Ecology and Environment of China., 2020. China National Urban Air Quality Real-Time Publishing Platform, https://datacenter.mee.gov.cn/ (last access 11th Nov. 2020).

Ministry of Land, Infrastructure, Transport and Tourism. 2017. http://www.mlit.go.jp/road/census/h27/index.html (last access 25th Jul. 2017).

Minoura, H., Takahashi, K., Chow, J. C. & Watson, J. G., 2006. Multi-year trend in fine and coarse particle mass, carbon, and ions in downtown Tokyo, Japan. Atmospheric Environment, 40(14), 2478-2487. https://doi.org/10.1016/j.atmosenv.2005.12.029.

Mori, T. & Notsu, K., 1997. Remote CO, COS, CO_2, SO_2, HCl detection and temperature estimation of volcanic gas. Geophysical Research Letters, 24(16), 2047-2050. https://doi.org/10.1029/97GL52058.

National Institute for Environmental Studies. 2020. https://www.nies.go.jp/igreen/tj_down.html (last access 1st Oct. 2020).

Nirmalkar, J., Batmunkh, T. & Jung, J., 2020. An optimized tracer-based approach for estimating organic carbon emissions from biomass burning in Ulaanbaatar, Mongolia. Atmospheric Chemical & Physics, 20,3231-3247. https://doi.org/10.5194/acp-20-3231-2020.

Olson, D. G., Tsuji, K. & Shiraishi, I., 2000. The reduction of gas phase air toxics from combustion and incineration sources using the MET–Mitsui–BF activated coke process. Fuel Processing Technology, 65, 393-405. https://doi.org/10.1016/S0378-3820(99)00106-X.

Pakkanen, T. A., Loukkola, K., Korhonen, C. H., Aurela, M., Mäkelä, T., Hillamo, R. E., Aarnio, P., Kousa, A. & Maenhaut, W., 2001. Sources and chemical composition of atmospheric fine and coarse particles in the Helsinki area. Atmospheric Environment, 35(32), 5381-5391. https://doi.org/10.1016/S1352-2310(01)00307-7.

Park, S.M., Seo, B.K., Lee, G., Kahng, S.H. & Jang, Y.W., 2015. Chemical composition of water soluble inorganic species in precipitation at Shihwa Basin, Korea. Atmosphere, 6(6), 732-750. https://doi.org/10.3390/atmos6060732.

Podolskaia, E., Ershov, D. & Kovganko, K., 2020. Automated construction of ground access routes for the management of regional forest fires. Journal of Forest Science, 66(8): 329–

338. https://doi.org/10.17221/59/2020-JFS.

Ren, X.H., Sun, H., Chi, H.H., Meng, X.X., Li, Y.P. & Levendis, Y.A. (2017). Hydrogen chloride emissions from combustion of raw and torrefied biomass. Fuel, 200: 37–46. https://doi.org/10.1016/j.fuel.2017.03.040.

Sickles, J.E. II, Hodson, L.L. & Vorburger, L.M., 1999. Evaluation of the filter pack for long-duration sampling of ambient air. Atmospheric Environment, 33, 2187-2202. https://doi.org/10.1016/S1352-2310(98)00425-7.

Sophie, C., 2019. Air Pollution in Mongolia. Bulletin of the World Health Organization, 97: 79–80. http://dx.doi.org/10.2471/BLT.19.020219.

Stein, A. F., Draxler, R. R., Rolph, G. D., Stunder, B. J., Cohen, M. D., & Ngan, F., 2015. NOAA's HYSPLIT atmospheric transport and dispersion modeling system. Bulletin of the American Meteorological Society, 96(12), 2059-2077.

Uchida, S., Kamo, H. & Kubota, H., 1988. The source of hydrogen chloride emission from municipal refuse incinerators. Industrial & Engineering Chemistry Research, 27, 2188-2190. https://doi.org/10.1021/ie00083a040.

Uchida, S., Kamo, H., Kubota, H. & Kanaya, K., 1983. Reaction kinetics of formation of hydrochloric acid in municipal refuse incinerators. Industrial & Engineering Chemistry Research, 22, 144-149. https://doi.org/10.1021/i200020a023.

Vogt, R.D., Guo, J., Luo, J., Peng, X., Xiang, R., Xiao, J. & Zhao, Y., 2007. Water chemistry in forested acid sensitive sites in sub-tropical Asia receiving acid rain and alkaline dust. Applied geochemistry, 22(6), 1140-1148. https://doi.org/10.1016/j.apgeochem.2007.03.005.

Wang, S.Q, Lee, W.B, Deng, X.J, Deng, T., Li, F. & Tan, H.B., 2015. Characteristics of air pollutant transport channels in Guangzhou region. China Environmental Science, 35(10), 2883-2890 (in Chinese).

Wang, Y.Q., Zhang X.Y. & Draxler, R.R., 2009. TrajStat: GIS-based software that uses various trajectory statistical analysis methods to identify potential sources from long-term air pollution measurement data. Environmental Modeling & Software, 24(8):938-939. DOI:10.1016/j.envsoft.2009.01.004.

Wey, M.Y., Liu, K.Y., Yu, W.J., Lin, C.L. & Chang, F.Y., 2008. Influences of chlorine content on emission of HCl and organic compounds in waste incineration using fluidized beds. Waste Management, 28, 406–415. https://doi.org/10.1016/j.wasman.2006.12.008.

Wilson , T.R.S., 1975. 'Salinity and the major elements of sea water', In: Riley, J.P., Skirrow, G (Eds.), Chemical Oceanography, 2nd Edition, Vol. 1. Academic Press, Orlando, pp. 365-413.

Wright, R.F., Norton, S.A., Brakke, D.F. & Frogner, T., 1988. Experimental verification of episodic acidification of freshwaters by sea salts. Nature, 334, 422–424.

Xiu, G., Zhang, D., Chen, J., Huang, X., Chen, Z., Guo, H. & Pan, J., 2004. Characterization of major water-soluble inorganic ions in size-fractionated particulate matters in Shanghai campus ambient air. Atmospheric Environment, 38(2), 227-236. https://doi.org/10.1016/j.atmosenv.2003.09.053.

Yang, X., Wang, T., Xia, M., Gao, X.M., Li, Q.Y., Zhang, N.W., Gao, Y., Lee, S.C., Wang, X.F., Xue, L.K., Yang, L.X. & Wang, W.X., 2018. Abundance and origin of fine particulate chloride in continental China. Science of the Total Environment, 624,1041-1051.

https://doi.org/10.1016/j.scitotenv.2017.12.205.

Yao, X., Chan, C. K., Fang, M., Cadle, S., Chan, T., Mulawa, P. & Ye, B., 2002. The water-soluble ionic composition of PM2. 5 in Shanghai and Beijing, China. Atmospheric Environment, *36*(26), 4223-4234. https://doi.org/10.1016/S1352-2310(02)00342-4.

Yao, X., Lau, A.P., Fang, M., Chan, C.K. & Hu, M., 2003. Size distributions and formation of ionic species in atmospheric particulate pollutants in Beijing, China: 1—inorganic ions. Atmospheric Environment, 37(21), 2991-3000. https://doi.org/10.1016/S1352-2310(03)00255-3.

Zhang, X., Murakami, T, Wang, J. & Aikawa, M., 2021. Sources, species and secondary formation of atmospheric aerosols and gaseous precursors in the suburb of Kitakyushu, Japan. Science of the Total Environment. https://doi.org/10.1016/j.scitotenv.2020.143001.

Zhang, X., Zhang, K., Liu, H., Lv, W., Aikawa, M., Liu, B. & Wang, J., 2020. Pollution sources of atmospheric fine particles and secondary aerosol characteristics in Beijing. Journal of Environmental Sciences, 95, 91-98. https://doi.org/10.1016/j.jes.2020.04.002.

Chapter 3 Methane concentration downtown and in the suburbs of an urbanized city and controlling parameters to determine its horizontal distribution

3.1 Introduction

Methane (CH_4) in the ambient air plays important roles from the viewpoint of climate change/global warming and also atmospheric chemistry. Methane is the second largest contributor to global warming, and its radiative forcing has been increasing (IPCC, 2007; 2013). In terms of atmospheric chemistry, CH_4 is involved in the photochemical formation of ozone, as it has been a significant air pollutant in recent years and one of the most important greenhouse gases. On the other hand, the time methane remains in the atmosphere is ca. 12 years (IPCC, 2007), meaning that methane has a moderate reactivity in the troposphere; therefore, it can be said to be a short-lived climatic pollutant (Ito et al., 2019). In contrast, when we look at methane from the standpoint of local air pollution, it is chemically stable/inactive in atmospheric chemistry, unlike photochemical oxidants and nitrogen oxides. Globally, methane has been emitted from both anthropogenic sources (56%) and natural sources (44%) (Saunois et al., 2020), of which fossil fuel production and use and agriculture and waste are roughly categorized as anthropogenic, while wetlands and other natural emissions are categorized as natural, and biomass and biofuel burning is categorized as natural and anthropogenic.

The methane concentration in the atmosphere is measured mainly for two purposes: (1) to evaluate climate change/global warming, and (2) to monitor local air pollution issues. As for the first purpose, methane is the second greatest contributor to global warming; thereby, not

only measuring but also evaluating the flux/budget is actively conducted, particularly in the region of Asia (e.g., Liu et al., 2007; Daelma et al., 2012; Dai et al., 2019; Crippa et al., 2020). Meanwhile, in terms of the second purpose, the primary target should be non-methane hydrocarbons (NMHCs), which are more actively involved in the production of air pollution due to their chemical activities, which are larger than those of methane. The methane concentration is determined as a separate byproduct. Literature that focuses on methane from the viewpoint of air pollution is quite rare. In particular, methane is seldom studied in urban areas from the standpoint of air pollution. The data on methane is, however, of value in atmospheric studies in urban areas, and methane can be an interesting indicator in atmospheric studies in urban area thanks to its relative inactivity in the field of atmospheric chemistry.

The stability of the atmosphere is a significant parameter for controlling the degree of air pollution. The NOx (NO + NO_2) and/or SPM (suspended particulate matter; 100% cut-off diameter is 10 mm) concentrations were severe during the winter season because of the complex effect of the primary emission, secondary production in the atmosphere, and the meteorological condition during the winter season (e.g., Cocks and Fletcher, 1989; Kimura and Aikawa, 1991; Kaneyasu et al., 1994, 2002; Yoshikado and Uosaki, 2000; Noble et al., 2003). In the studies vigorously investigated, the targets were focused on air pollutants such as nitrogen oxides, particulate matter, and photochemical oxidants. These target substances are generally and chemically unstable in the atmosphere. In contrast, Aikawa et al. (1996; 2006) studied the vertical atmospheric structure related to heat island intensity and atmospheric stability in urban areas by using the dataset of the methane concentration and air temperature. Due to relatively less chemical reactiveness, the conversion from methane to other chemical compounds can be

relatively neglected as compared with the air pollutants shown above. Aikawa et al. (1996) found the symbolic diurnal variation and its seasonality in the methane concentration and discussed the relation with vertical atmospheric stability in the central part of a megacity in Japan. Further, they deepened the study associated with heat island intensity (Aikawa et al., 2006).

We tried to evaluate the similarity/difference in the relation between the diurnal variation of the methane concentration and atmospheric conditions in an urban area different from those studied previously. The areas in the former studies were flat without large hills/mountains. In contrast, the target area in this study forms one economic zone but complexly includes a bay as well as a mountain. In this study, we could find the unique diurnal variation in the methane concentration and comprehensively elucidate the kinetic behavior of methane in the urban atmosphere in not only the central part of a big city but also its suburbs.

3.2 Experimental

3.2.1 Location and classification of sites

Methane concentrations determined at three sites (Egawa, Kitakyushu, and Mihagino) in Kitakyushu City were statistically analyzed. The locations of the three sites are shown in Fig. 3-1, and detailed information on the sites is summarized in Table 3-1. Kitakyushu City is one of the most industrialized cities in Japan, and its population density is more than 961,000 people/492 km^2. The Kitakyushu site and the Mihagino site are located in the central and downtown area of the city, having already been developed; in contrast, the Egawa site is in the suburbs of the city and is still being developed as new residential area.

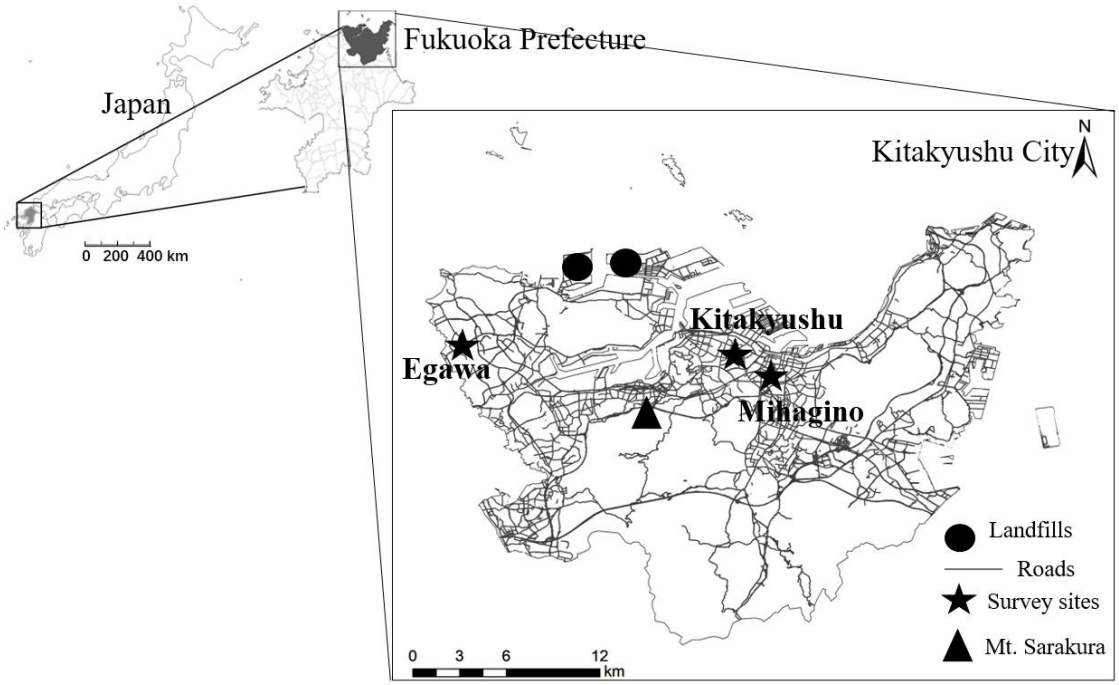

Fig. 3-1. Location of survey area and sites.

Table 3-1 Information of three sites.

No.	Name	Latitude	Longitude	Feature of target air	Use district of surroundings	Attribution
1	**Egawa**	**33.893564°N**	**130.693230°E**	**General ambient air**	**Residential**	**Suburban/Rural**
2	**Kitakyushu**	**33.886413°N**	**130.850429°E**	**General ambient air**	**Residential**	**Urban**
3	**Mihagino**	**33.872644°N**	**130.880491°E**	**Roadside air**	**Commercial**	**Urban**

3.2.2 Methane concentration

The methane concentration statistically analyzed in the study was determined by the City of Kitakyushu and obtained through the web site of the Ministry of the Environment, Japan (MOE, 2021). The non-methane hydrocarbon concentration simultaneously determined with the methane concentration was also used in the statistical analyses as a typical indicator of

automobile emissions. A one-year data set from March 1, 2018, to February 28, 2019, was used for the statistical analyses. In one year, the data for 25 days (April 21 to 23, November 29 and 30, and February 9 to 28) were missing; taking into account the missing data on air temperature (section 3.2.3), a total of 313 days (spring: 87 days; summer: 70; autumn: 86; and winter: 70) were statistically analyzed for each site. Determining the data for analysis, only days missing information for less than 4 of 24 hours were used.

3.2.3 Vertical air temperature

The City of Kitakyushu is continuing to measure air temperature at six different heights (140, 190, 265, 345, 445, and 545 m above sea level (a.s.l.)) by installing a ventilating type of thermometer at Mt. Sarakura (Summit: 622 m a.s.l.). Mt. Sarakura is located near the central part of Kitakyushu City (Fig. 3-1). Air temperature data were used to study the atmospheric stability from the viewpoint of the formation of the temperature inversion layer around the central part of Kitakyushu City. In a one-year data set corresponding to the methane concentration, the data for 27 days (March 5, 7, June 29, 30, July 1–20, and November 22–24) were missing, with the result that 339 days (spring: 90 days; summer: 70; autumn: 89; and winter: 90) were statistically analyzed for each height.

The University of Kitakyushu is measuring air temperature at two heights (on the ground and on the rooftop of the school building; ca. 20 m above the ground). The thermometer was put in a wooden shelter without a ventilation system. The shelter at ground level was located on the northern side of the school building; therefore, the shelter was in shadows during the daytime. On the other hand, the shelter on the rooftop was in the sunshine during the daytime, indicating

that the two thermometers would show a difference in the observation results attributable to the discrimination of the shelter stand.

3.2.4 Land use

The land use around the site is an important parameter for determining and understanding the atmospheric conditions in terms of the methane concentration as well as the atmospheric stability. The land-use data prepared by the Ministry of Land, Infrastructure, Transport and Tourism, Japan (MLIT, 2021) was used in the analysis.

3.2.5 Seasonal classification

In the seasonal analyses, the seasons were defined as follows: spring—March, April, and May; summer—June, July, and August; autumn—September, October, and November; winter—December, January, and February.

3.3 Results and Discussion

3.3.1 Diurnal variation

Figure 3-2(a) shows the annual diurnal variation of the CH_4 concentrations at the three sites; the CH_4 concentrations were higher at night and lower during the day at all sites. The same diurnal variation was shown in the study by Aikawa et al. (1996), although both the time and the site were different from those of this study. Aikawa et al. (1996) demonstrated the monthly variation of the CH_4 concentration in detail and its harmonized relationship with the formation of the elevated temperature inversion layer.

A clear difference was observed among the three sites; whereas there existed little difference in

the diurnal variations at Kitakyushu and Mihagino, Egawa showed a clear difference from other two sites. A clear difference between Egawa and the other two sites (Kitakyushu and Mihagino) appeared during the daytime. The diurnal variation at Egawa showed a clear minimum at 16:00; in contrast, those at Kitakyushu and Mihagino did not, instead keeping a constant level from 13:00 to 17:00. For this clear difference during the day between Egawa and Kitakyushu and Mihagino, the two dominant contributing factors mentioned below would be involved.

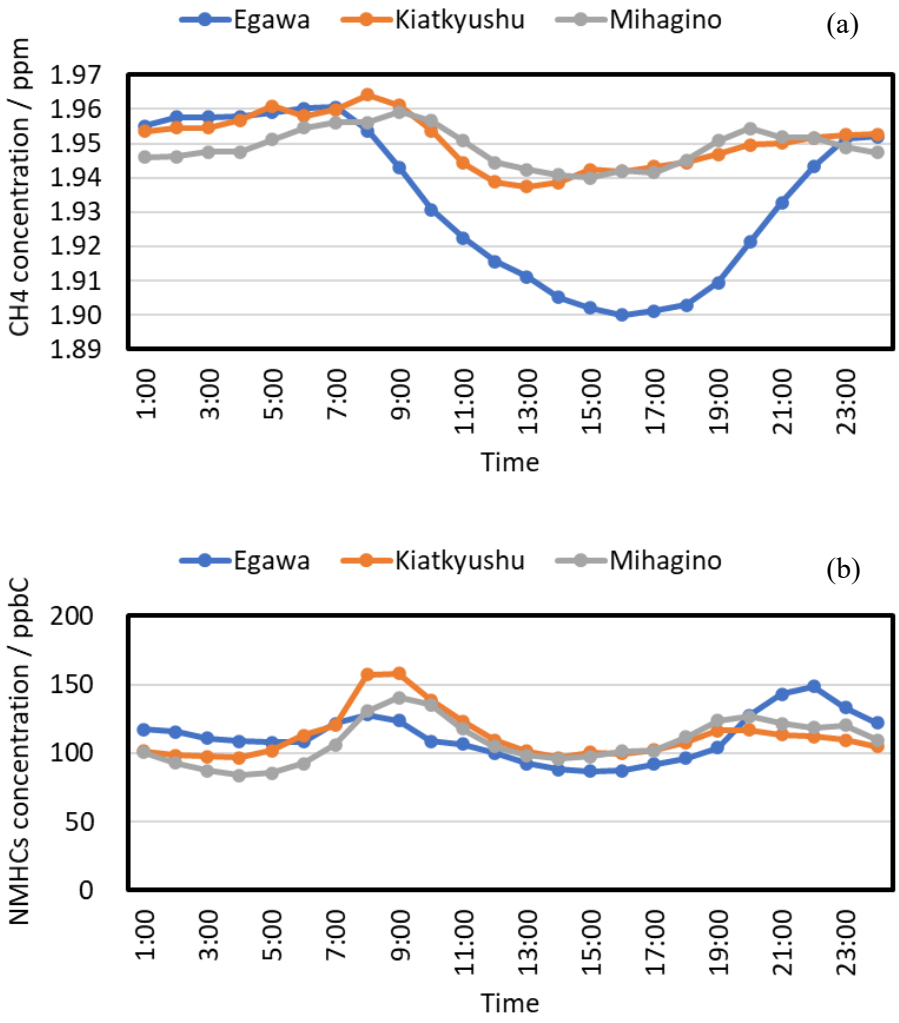

Fig. 3-2. Annual diurnal variation of the CH_4 (a) and non-methane hydrocarbons (NMHCs) (b) concentrations at three sites.

First, landfills were contributors to Kitakyushu and Mihagino but not to Egawa in daytime. Fig. 3-3(a) and (b) show the wind rose during the day (12:00–17:00) and at night (0:00–5:00) in Kitakyushu City, respectively, as observed by the Japan Meteorological Agency. The wind direction during the day was distinguishably different from that at night, most certainly due to the land/sea breeze. Furthermore, as shown in Fig. 3-1, landfills are located on the windward side of the sites of Kitakyushu and Mihagino during the day. Landfill is an influential source of CH_4 emissions (IPCC, 2007; 2013); thus, the advection from landfill to the two sites during the day would characteristically prevent the CH_4 concentrations at Kitakyushu and Mihagino from decreasing during the day.

Automobiles are a second dominant contributor. This will be discussed in the next section (section 3.3.2) in detail associated with the diurnal variation of the NMHC concentration.

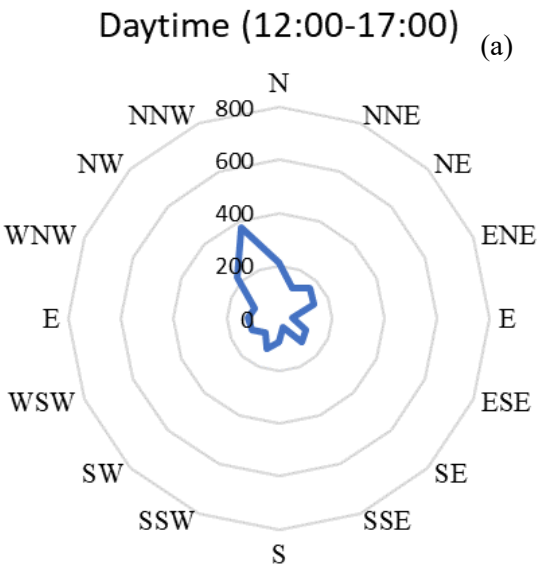

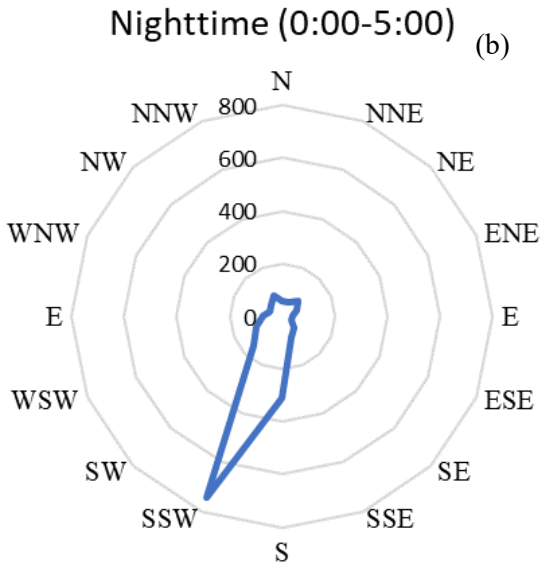

Fig. 3-3. Wind rose in daytime (12:00-17:00) (a) and nighttime (0:00-5:00) (b) in Kitakyushu City based on the data observed at Yahata by Japan Meteorological Agency. The number of axis is the number of hour.

3.3.2 Variation at midnight and temperature inversion layer

Figure 3-2 (b) shows the diurnal variation of the NMHC concentrations at the three sites. We should pay attention to the NMHC concentrations from midnight to early morning. The NMHC concentration was higher at Egawa than at Kitakyushu and Mihagino despite NMHCs being an indicator of automobile emissions and the fact that Egawa is a suburban site. This strongly indicates the stronger atmosphere stability at Egawa, i.e., the formation of a grounded temperature inversion layer. Aikawa et al. (1996; 2006) demonstrated the formation of the temperature inversion layer in the urban area; here, it should be carefully noted that the temperature inversion layer they demonstrated was elevated above the ground, not grounded. A temperature inversion layer is generally formed at the ground, but in the central area studied by Aikawa et al. (1996; 2006), it is frequently formed above the ground—a so-called elevated

temperature inversion layer—due to anthropogenic heat emission producing a heat island effect. When we look at the NMHC concentration from midnight to early morning, taking the grounded temperature inversion layer formed at only suburban (Egawa) and the elevated temperature inversion layer in the central city areas (Kitakyushu and Mihagino) into account makes it possible to explain the higher NMHC concentration at Egawa than those at Kitakyushu and Mihagino due to effective condensation in spite of fewer emissions of NMHCs at Egawa. The formation and existence of the grounded and elevated temperature inversion layers will be shown and discussed in detail in section 3.3.5.

The similar phenomenon could be applied to the CH_4 concentration from midnight to early morning, i.e., the CH_4 concentration at Egawa was higher than or equivalent to those at Mihagino and Kitakyushu, respectively. Methane is not a typical indicator of automobiles, and the flux/emission from automobiles is not a major contributor on a global scale; however, in urban areas, CH_4 is not negligible, as has been shown in previous studies (Aikawa et al., 1996; 2006). The importance of CH_4 emissions appearing in two peaks will be shown in the next section (section 3.3.3).

3.3.3 Two peaks in the early morning and evening

3.3.3.1 Early morning peak

Two peaks were observed in the early morning and evening in the diurnal variation of the CH_4 concentration (Fig. 3-2(a)).

The time when the peak appeared in the early morning had a time gap of one hour among the three sites: 7:00 at Egawa, 8:00 at Kitakyushu, and 9:00 at Mihagino. Globally speaking, CH_4

emissions from automobile are not of importance; however, it should not be neglected around urban areas because other sources of CH_4 emissions, such as fuel production, agriculture, and waste, which are major contributors on a global scale, exist infrequently in urban areas (Aikawa et al., 1996). The one-hour gap in the peak time among the three sites is qualitatively consistent with the traffic stream from the suburbs to the central/downtown area of the city in the morning. The reason for the gap in the peak due to the traffic stream among the three sites is supported by the diurnal variation of the NMHC concentration (Fig. 3-2(b)), which is an indicator of automobile emissions.

3.3.3.2 Evening peak

A shoulder peak was observed at Mihagino in the evening; in contrast, little peak was observed at Kitakyushu, although they are both located in the central area. This is first due to the difference in the target air (Table 3-1); secondly, the evening rush hour is less deconcentrated as compared with that in the early morning. Actually, the peak of the NMHC concentration in the evening was broader than that in the early morning, even at Mihagino. The diurnal variation at Egawa was clearly different from those at Kitakyushu and Mihagino. The reasons for this difference only at Egawa have already been discussed in sections 3.3.1 and 3.3.2.

3.3.4 Seasonal diurnal variations at each site

Fig. 3-4(a)–(d) show the diurnal variations at the three sites in spring, summer, autumn, and winter, respectively. At all sites, the seasonal mean concentration was controlled on a global scale; it was lower in summer and higher in winter. In contrast, the difference among the three sites was first observed as the discrepancy between Egawa and Kitakyushu and Mihagino,

defined as the concentration gap between the maximum and minimum concentrations in the diurnal variation. The concentration gaps (Δ) are listed in Table3- 2. The values of Δ at Egawa in spring and summer were larger than or comparable to those in autumn and winter, whereas those at Kitakyushu and Mihagino in spring and summer were smaller than those in autumn and winter; in other words, little diurnal variation was observed at Kitakyushu and Mihagino in spring and summer (Figs. 3-4(a) and (b)). A smaller diurnal variation in a warmer season than in a colder season in this study accords with the results of other studies (Aikawa et al., 1996; 2006), in which they referred to the relation of the diurnal variation to the vertical atmospheric stability, i.e., the existence of elevated temperature inversion layer. The second difference among the three sites appeared in the hours from midnight to sunrise during the summer; the CH_4 concentration at Egawa was distinguishably higher than those at Kitakyushu and Mihagino. These points will be considered and discussed in detail later (sections 3.3.5 and 3.3.6) in relation to the formation of temperature inversion layers and land use

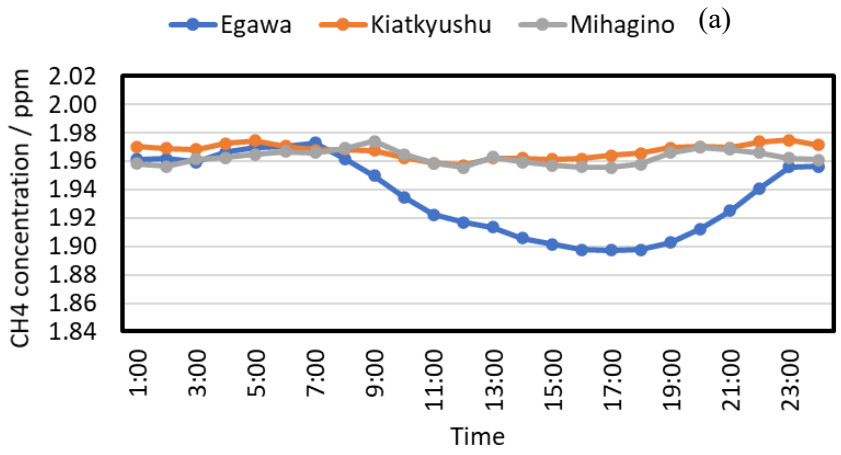

.

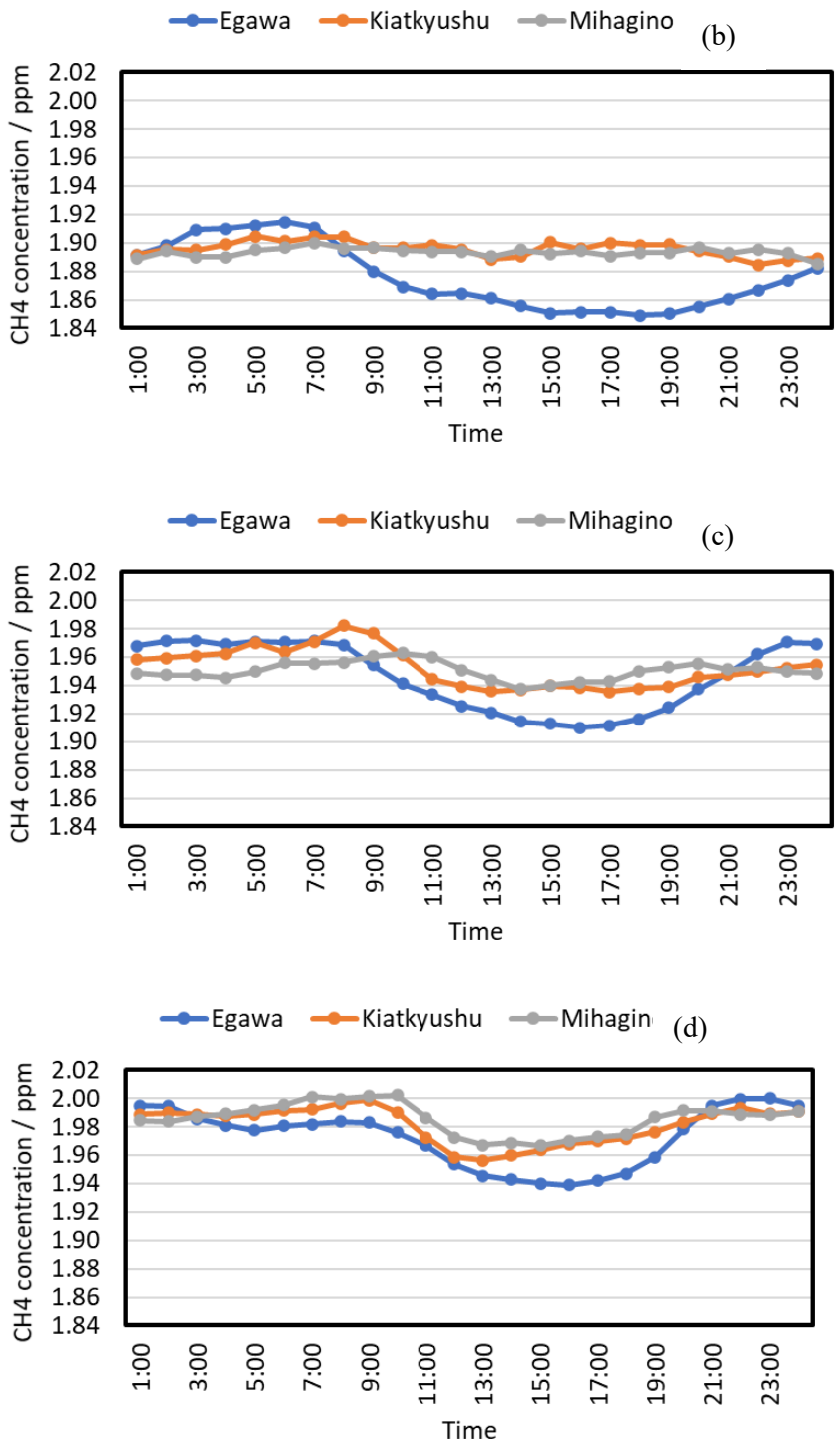

Fig. 3-4. Diurnal variation of the CH_4 concentration at three sites in spring (a), summer (b), autumn (c) and winter (d).

Table 3-2 Concentration gap (Δ) between maximum and minimum in diurnal variation

	Δ / ppm			
	Spring	**Summer**	**Autumn**	**Winter**
Egawa	**0.075**	**0.065**	**0.062**	**0.063**
Kitakyushu	**0.017**	**0.021**	**0.046**	**0.042**
Mihagino	**0.018**	**0.015**	**0.027**	**0.035**

3.3.5 Vertical profile of air temperature

3.3.5.1 Central city

Figures 3-5(a)–(c) show the differences in air temperature between 190 m and 140 m (190 minus 140 m), 265 m and 190 m (265 minus 190 m), and 345 m and 265 m (345 minus 265 m), respectively, in August and January, in which the gray zone indicates that the atmosphere is stable when considering the adiabatic lapse rate (-1°C/100 m). The atmosphere over the central city was thermally unstable under a height of 190 m, indicating that not only the air but also air pollutants are vertically mixed by convection. In contrast, the atmosphere over 190 m was stable. Furthermore, a temperature inversion layer was formed except for several hours in August, indicating that an elevated temperature inversion layer suppresses convection at a height of ca. 200 m. It is noteworthy that the temperature inversion layer was formed even in August, i.e., the hottest month in Japan, and even during the day, except for several hours. Aikawa et al. (1996) showed the formation of a similar elevated temperature inversion layer in the central part of Nagoya City, whose population density is more than 2,300,000 people/326.5 km^2; however, the elevated temperature inversion layer in August in Nagoya City demonstrated by

Aikawa et al. (1996) was quite limited only for the hour in the early morning. A vertical profile of air temperature over the central city strongly suggests that the elevated temperature inversion layer, which inhibits the diffusion/transportation of air pollutants, is likewise formed over other developed cities; however, its seasonality is different. The elevated temperature inversion layer in Kitakyushu City is more frequently and strongly formed and has a strong and deep influence on the diurnal variation of air pollutants in Kitakyushu City.

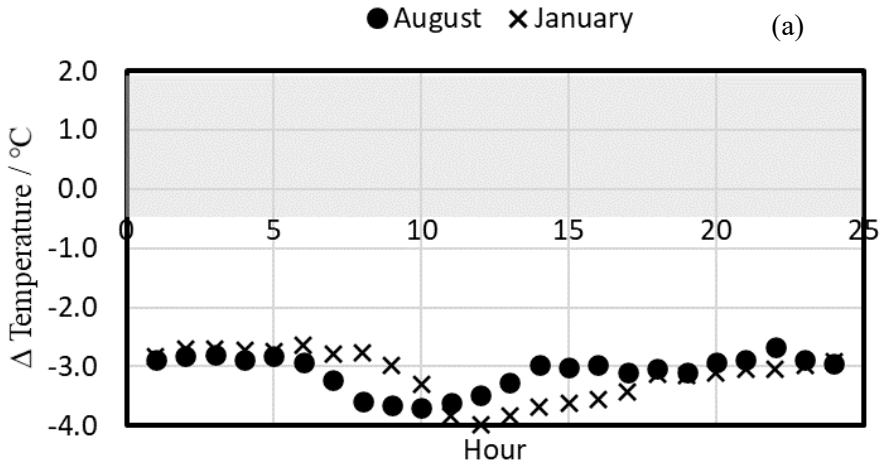

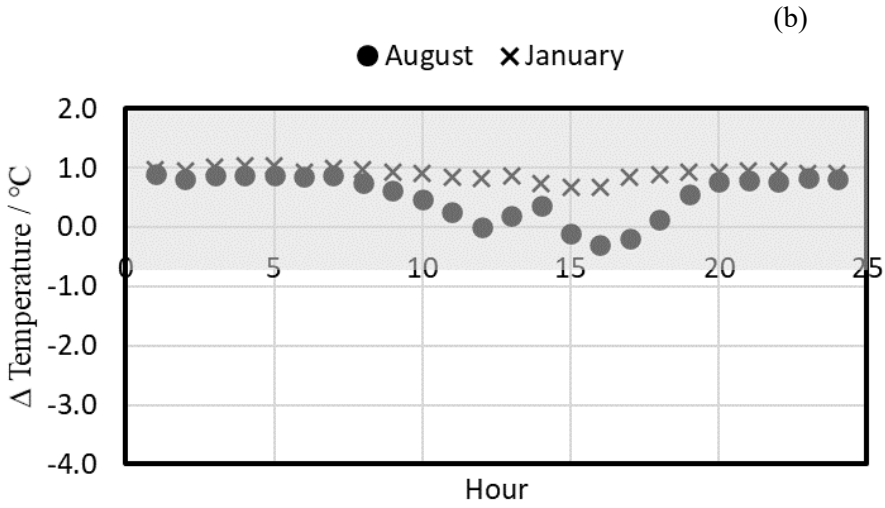

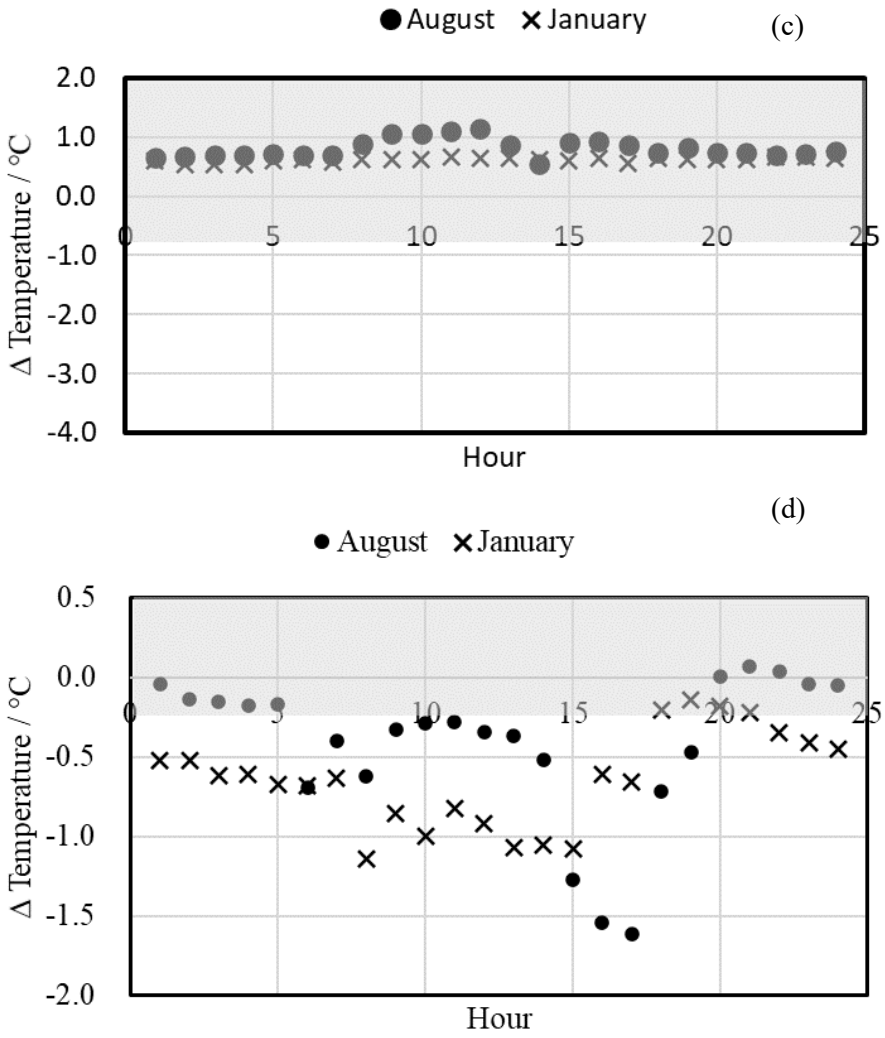

Fig. 3-5. Difference (Δ) of the air temperature between 190 m and 140 m (190 m minus 140 m) (a), 265 m and 190 m (265 m minus 190 m) (b), and 345 m and 265 m (345 m minus 265 m) (c) at Mt. Sarakura, and between rooftop (ca. 20 m above the ground) and ground in suburbs (d). Gray zone indicates that the atmosphere is stable in taking the adiabatic lapse rate (-1°C / 100 m) into account.

3.3.5.2 Suburbs

The vertical profile of air temperature in the suburbs, i.e., the University of Kitakyushu, is difficult to evaluate because the results at two heights are different due to the discrimination of the shelter stands. To elucidate the vertical profile of air temperature, we tried to correct the observation results on the rooftop during the day as follows, assuming that the air temperature recorded on the rooftop would be higher than that if the wooden shelter had been in shadows:

(1) for 2 hours after sunrise and before sunset; corrected air temperature on the rooftop [°C] = recorded air temperature [°C]–0.5 [°C];

(2) for the daytime hours except (1); corrected air temperature on the rooftop [°C] = recorded air temperature [°C]–1 [°C].

This correction factor is determined based on the information reported by Imai et al. (2021).

Figure 3-5(d) shows the difference in air temperature between the ground level and the height of 20 m above the ground in August and January at the University of Kitakyushu, in which the gray zone indicates that the atmosphere is stable, in the same manner as shown in Fig. 3-5(a)–(c). The vertical profile of air temperature in the suburbs (Fig. 5(d)) indicated some features, as follows:

(1) the atmosphere less than 20 m above the ground in the suburbs was unstable during the day in both summer and winter;

(2) it was unstable even at night in the winter; in contrast, it was stable at night in summer.

Those features strongly suggest that the grounded temperature inversion layer was formed at night in summer in the suburbs. That the atmosphere below 20 m above the ground was unstable all day during winter is quite interesting and is partially and likely due to the strong

northwestern wind; actually, the monthly mean wind velocity and the maximum daily mean wind velocity in August 2018, i.e., in summer, observed near the University of Kitakyushu were 1.2 m/s and 2.7 m/s, respectively. In contrast, those in January 2019, i.e., in winter, were 1.8 and 4.3, respectively (City of Kitakyushu, 2019).

3.3.6 Relation to land use

Figures 3-6(a) show the land use reflecting ca. the 3 km x ca. 3 km region around Egawa, Kitakyushu, and Mihagino, respectively. Clear differences were observed among the three sites. Whereas the land use around Kitakyushu and Mihagino was similar, Egawa showed a clear difference from other two sites, being the same as the grouping in the diurnal variation (section 3.3.1). From the standpoint of CH_4 emissions, the most significant difference appears in paddy fields; ca. 8% of the area around Egawa was occupied by paddy fields, but there was none around Kitakyushu and Mihagino. Methane is generated and released to the atmosphere from submerged paddy fields, corresponding to the summer season in Japan.

(a)

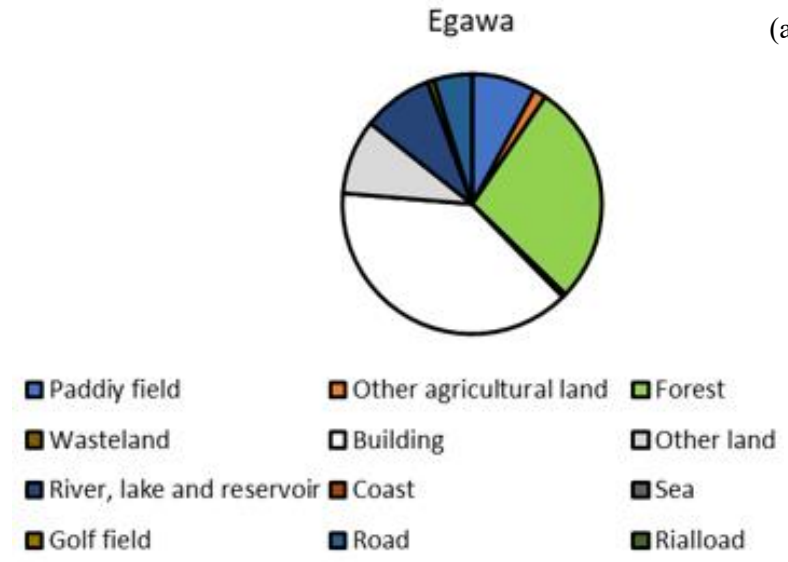
Egawa
Paddiy field
Other agricultural land
Forest
Wasteland
Building
Other land
River, lake and reservoir
Coast
Sea
Golf field
Road
Rialload

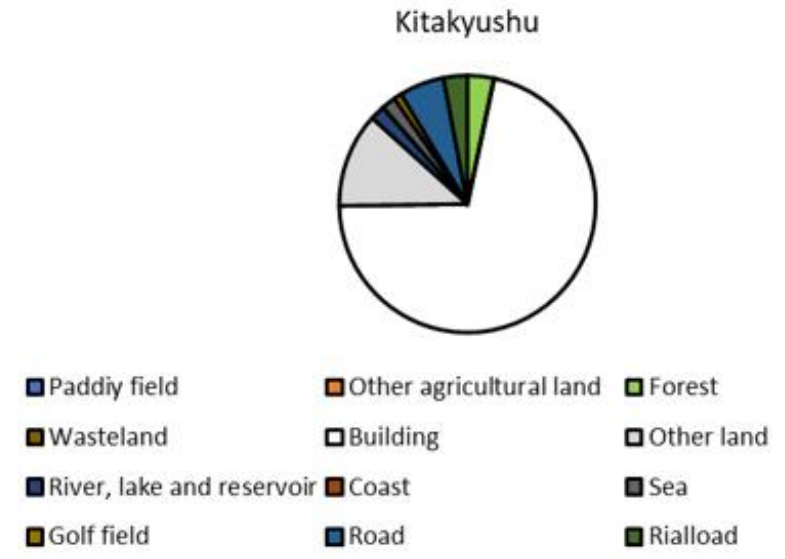
Kitakyushu
Paddiy field
Other agricultural land
Forest
Wasteland
Building
Other land
River, lake and reservoir
Coast
Sea
Golf field
Road
Rialload

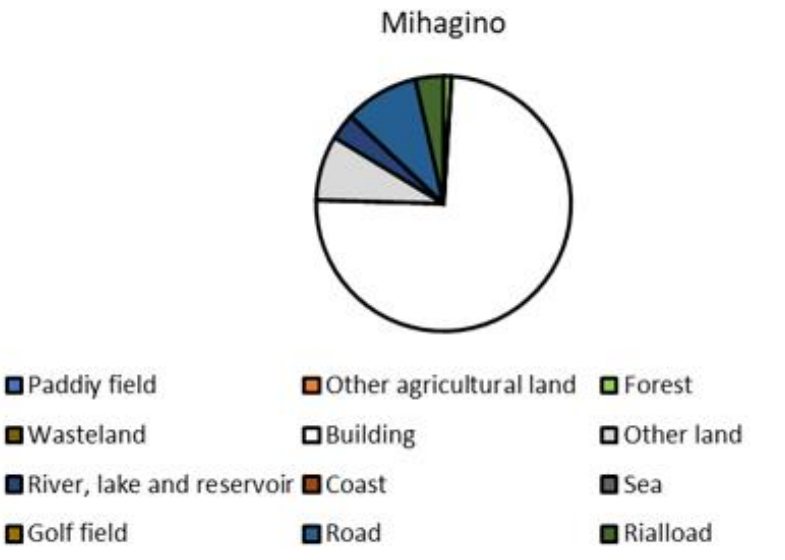
Mihagino
Paddiy field
Other agricultural land
Forest
Wasteland
Building
Other land
River, lake and reservoir
Coast
Sea
Golf field
Road
Rialload

(b)

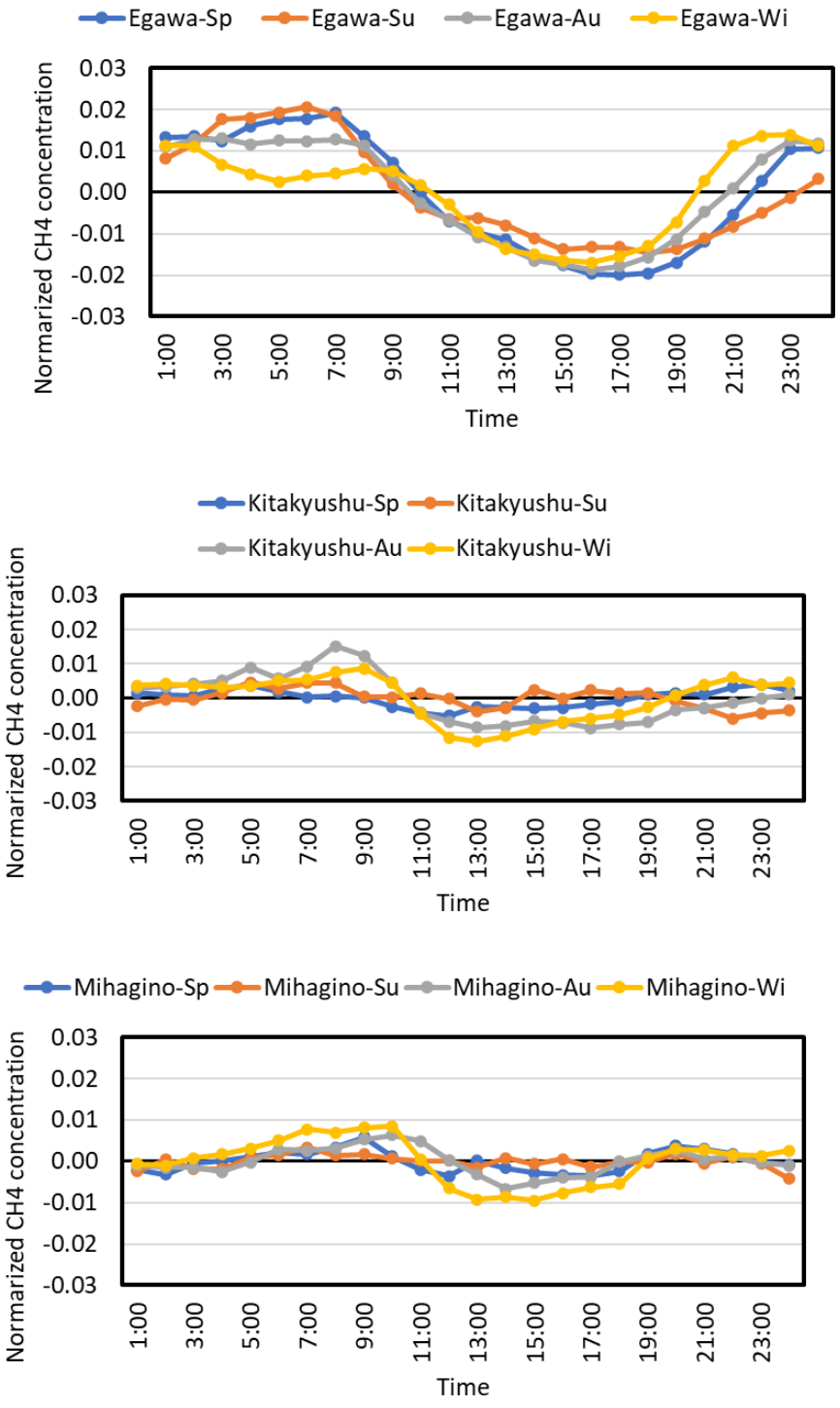

Fig. 3-6. Land use reflecting ca. 3 km x ca. 3 km region around three sites (a), and normarized diurnal variation of CH_4 concentration in each season at three sites (b). Value in vertical axis shows the ratio of the CH_4 concentration at each hour to seasonal mean.

Figures 3-6(b) show the normalized diurnal variation of CH_4 concentrations each season at Egawa, Kitakyushu, and Mihagino, respectively, where the CH_4 concentration at each hour is divided by the seasonal mean to cancel the difference in the CH_4 concentration due to not only the season but also the site and to make comparison easy. As shown in Fig. 3-2(a), the CH_4 concentration at Egawa varied more in a day than did those at Kitakyushu and Mihagino. In addition, some clear, pronounced, and interesting distinctions among the seasons were observed at Egawa during the hours from early evening to early morning. First, the hour when the CH_4 concentration was above the seasonal mean in the early evening had a clear order—winter was the earliest, followed by autumn, spring, and summer. Second, the CH_4 concentration in the early morning (3:00–6:00) was the highest in summer, although the hour at which it started increasing was latest in the evening. These two would be closely related to CH_4 flux/emission and the stability of the atmosphere around the site. Around the Egawa site, paddy fields occupied ca. 8% of the land; furthermore, the atmosphere around Egawa was stabilized at night during the summer (section 3.3.5.2). The compositive mechanism likely produced the discriminating diurnal variation at Egawa, unlike those at Kitakyushu and Mihagino.

The CH_4 concentrations at Kitakyushu and Mihagino at night were higher in colder seasons (autumn and winter) than in warmer seasons, whereas the opposite situation occurred at Egawa, as shown above. Furthermore, the CH_4 concentration from midnight to early morning at Egawa in the winter was emphatically lower than those in the other three seasons, presumably providing information as to the emission sources of CH_4 as follows: (1) there is a fixed quantity of flux/emissions in urban areas, and the contribution from automobiles could not be negligible; and (2) a seasonally specific flux/emission from paddy fields in summer dominantly contributes

if paddy fields remain in the suburbs.

3.4 Conclusion

The CH_4 concentrations observed in an industrialized city, Kitakyushu City, in Japan were statistically analyzed to elucidate the contributing factors so as to control its diurnal variation and further its seasonality. In addition to the previous works, the differences between a suburbs and a downtown of one of the largest and industrialized cities in Japan were studied in detail. The CH_4 concentrations showed the typical diurnal variation—lower during the day and higher at night. While the seasonal CH_4 concentration was controlled on a global scale—lower in summer and higher in winter—the diurnal variation showed some seasonally distinguishing patterns: (1) the gap between the maximum and minimum concentrations in the diurnal variation was small in the central area and large in the suburbs; (2) two peaks attributable to automobiles were observed, especially in the central area, clearly and the time when the peak appeared showed a time gap of one hour among the three sites during morning rush hour; (3) the CH_4 concentration in the suburbs in summer was higher than that in the central area, thanks to the complex influence of flux/emissions from paddy fields and the formation of a grounded temperature inversion layer.

References

Aikawa, M., Yoshikawa, K., Tomida, M., Haraguchi, H., 1996. Characteristic behaviors of the methane concentrations in urban atmosphere of Nagoya with relation to atmospheric stability. *Environmental Sciences* **9(2)**, 201–210.

Aikawa, M., Hiraki, T., Eiho, J., 2006. Vertical atmospheric structure estimated by heat island intensity and temporal variations of methane concentrations in ambient air in an urban area in Japan. *Atmospheric Environment* **40**, 4308-4315. doi:10.1016/j.atmosenv.2006.03.044

City of Kitakyushu, 2019. White paper on Environment. https://www.city.kitakyushu.lg.jp/kankyou/00101200.html (last access: May 29th, 2021).

Cocks, A.T., Fletcher I.S., 1989. Major factors influencing gas-phase chemistry in power plant plumes during long range transport-II. Release time and dispersion rate for dispersion into an 'urban' ambient atmosphere. *Atmospheric Environment* **23**, 2801-2812.

Crippa, M., Solazzo, E., Huang, G., Guizzardi, D., Koffi, E., Muntean, M., Schieberle, C., Friedrich, R., Janssens-Maenhout, G., 2020. High resolution temporal profiles in the emissions database for global atmospheric research. Sci. Data 7, 121.

Daelman, M.R.J., van Voorthuizen, E.M., van Dongen, U.G.J.M., Volcke, E.I.P., van Loosdrecht, M.C.M., 2012. Methane emission during municipal wastewater treatment. Water Res. 46, 3657–3670.

Dai, S., Ju, W., Zhang, Y., He, Q., Song, L., Li, J., 2019. Variations and drivers of methane fluxes from a rice-wheat rotation agroecosystem in eastern China at seasonal and diurnal scales. *Science of the Total Environment* 690, 973–990.

Imai, M, Sakakibara, N., Jitsumori, A., 2021.

https://testbed.nict.go.jp/jgn/jgn2_archive/japanese/08-library/meeting_doc/data/WS-11/2-5-imai.pdf (last access: Dec. 5th, 2021)

Intergovernmental Panel on Climate Change (IPCC), 2007. Climate Change 2007: The Physical Science Basis. Cambridge University Press

Intergovernmental Panel on Climate Change (IPCC), 2013. Climate Change 2013: The Physical Science Basis. Cambridge University Press

Ito, A., Tohjima, Y., Saito, T., Umezawa, T., Hajima, T., Hirata, R., Saito, M, Terao, Y., 2019. Methane budget of East Asia, 1990–2015: A bottom-up evaluation. *Science of the Total Environment* **676**, 40–52.

Kaneyasu, N., Yoshikado, H., Mizuno, T., Tanaka, T., Sakamoto, K., Wang, Q.Y., Sofuku, M., 1994. Wintertime photochemical air pollution as a cause of heavy NO_2 pollution in Kanto Plain, Japan. *Journal of Japan Society of Air Pollution* 29(2), 80-91. (in Japanese with English abstract)

Kaneyasu, N., Yoshikado, H., Kondo, H., Moriya, T., Suzuki, M., Shirakawa, Y., 2002. Modeling of suspended particulate matter during early-winter severe pollution episodes (I): Development of an emission source model. *Journal of Japan Society for Atmospheric Environment* 37(3), 167-183. (in Japanese with English abstract)

Kimura, F., Aikawa, M., 1991. Formation mechanisms of NO_2 in urban area in the cold half year. *Tenki* 38(5), 61-69. (in Japanese)

Liu, L., Zhou, L., Wen, M., Zhang, F., Fang, S., Yao, B., 2009. Characteristics of atmospheric CH_4 concentration variations at four national baseline observatories in China. Advances in Climate Change Research 5, 285–290. (in Chinese with English abstract)

MILT, 2021. National Land Information Division, National Spatial Planning and Regional Policy Bureau, MLIT of Japan. https://nlftp.mlit.go.jp/ksj/jpgis/jpgis_datalist.html (last access: May 16th, 2021).

MOE, 2021. Ministry of the Environment, Japan. http://www.env.go.jp/air/osen/report/index.html (last access: May 16th, 2021).

Noble, C.A., Mukerjee, S., Gonzales, M., Rodes, C.E., Lawless, P.A., Natarajan, S., Myers, E.A., Norris, G.A., Smith, L., Özkaynak, H., Neas, L.M., 2003. Continuous measurement of fine and ultrafine particulate matter, criteria pollutants and meteorological conditions in urban El Paso, Texas. *Atmospheric Environment* **37**, 27-840.

Saunois, M., et al., 2020. The Global Methane Budget 2000–2017. *Earth System Science Data* **12**, 1561–1623. https://doi.org/10.5194/essd-12-1561-2020

Yoshikado, H., Uosaki, K., 2000. Severe air pollution in early winter in the Nobi Plain Areas - Differences in meteorological structure compared with the Kanto District-. *Journal of Japan Society for Atmospheric Environment* 35(1), 63-75. (in Japanese with English abstract)

Chapter 4 Conclusion and Future Prospect

4.1 Conclusion

This study investigated the effects of transboundary air pollution and meteorological factors on air quality in the northern Kyushu region of Japan. Temporal variations of anthropogenic/nss-Cl and CH_4 concentrations, transboundary air pollution and meteorological effects on air quality from 2016 to 2019 in northern Kyushu, Japan, i.e., Kitakyushu city area.

a) The presence of anthropogenic/nss-Cl was observed on 263 of 365 days, consecutive sampling from December 2016 to November 2017 at the University of Kitakyushu. Among them, anthropogenic/nss-Cl concentrations were higher than 20 $nmol \cdot m^{-3}$ on 50 days.

b) High anthropogenic/nss-Cl concentrations were predominant in the north wind direction, while high concentrations were rare in the south wind direction. The active volcanoes in Japan are located south of the University, suggesting that domestic volcanoes have little effect on the concentration of anthropogenic/nss-Cl.

c) The correlation between anthropogenic/nss-Cl concentrations and meteorological conditions (wind speed) was low (the Pearson correlation coefficient: -0.09 ($p>0.05$)), indicating that municipal waste incineration and domestic coal combustion contributed little to high concentrations of anthropogenic/nss-Cl.

d) The 72-h backward trajectory results indicate that the study area is generally influenced by northwesterly and northerly winds, with transboundary transport from northeastern and southern regions of China, Mongolia, Russia, and the Sea of Japan contributing significantly to the high concentrations of anthropogenic/nss-Cl at the University. Thus,

air pollutants can arrive in northern Kyushu, Japan, through transboundary transport, affecting local air quality.

e) In both the suburbs (Egawa) and the city center (Kitakyushu and Mihagino) of one of the largest industrialized cities in Japan, methane concentrations show typical diurnal variation, i.e., higher at night than during the day.

f) The diurnal variation in the Egawa shows a clear minimum at 16:00; in contrast, Kitakyushu and Mihagino do not but remain at a constant level from 13:00 to 17:00. Based on the wind rose polar of Kitakyushu during the daytime (12:00-17:00) and nighttime (0:00-5:00), it was found that the landfill is located on the windward side of the Kitakyushu and Mihagino sites during the daytime. Therefore, advection from the landfill to these two sites during the daytime would prevent CH_4 concentrations at Kitakyushu and Mihagino from decreasing during the day.

g) All three sites showed peaks in the early morning, at 7:00 a.m. in Egawa, 8:00 a.m. in Kitakyushu, and 9:00 a.m. in Mihagino; the one-hour gap in peak time between the three sites was consistent with the qualitative traffic stream from the suburbs to the city center/downtown in the morning. Combined with the diurnal variation of NMHC concentrations as an indicator of automobile emissions, it supports that the traffic stream causes the peak methane concentration gap between the three sites.

h) The CH_4 concentration in the suburban area (Egawa) was higher than that in the central urban area (Kitakyushu and Mihagino) from midnight to early morning, mainly due to a grounded temperature inversion layer in the suburban area, where effective condensation is more pronounced.

i) Seasonal variations in CH_4 concentrations at the three sites are controlled on a global scale, i.e., lower in summer and higher in winter. In contrast, the CH_4 concentration gap values in spring and summer at Egawa were more significant than or comparable to those in fall and winter. In comparison, the CH_4 concentration gap values in spring and summer at Kitakyushu and Mihagino were smaller than those in fall and winter.

j) In the central urban area, the diurnal variation in the warm season in this study was smaller than that in the cold season, which is consistent with the results of other studies, mainly the relationship between daily variation and vertical atmospheric stability, i.e., the presence of a high-temperature inversion layer.

k) CH_4 concentrations in the suburbs in summer were higher than those in the central region because of the complex influence of fluxes/emissions from rice paddies and the formation of a grounded inversion layer. The atmosphere around Egawa was stable on summer nights, i.e., the formation of a grounded inversion layer; paddy fields around Egawa occupy ca. 8% of the area, and the flooded paddy fields release CH_4 into the atmosphere in summer.

Therefore, the air quality in the study area was dominated by 1) transboundary pollution was one of the main pollution sources in the survey site, which affects the local air quality; 2) local meteorological conditions cause the formation of a temperature inversion layer in both urban and suburban areas, which inhibits the transport of local pollutants and affects the survey site's air quality.

4.2 Future Prospect

Air pollution and climate change are inextricably connected and interact. Air pollutants include much more than greenhouse gases like carbon dioxide (CO_2), methane, and nitrous oxide (N_2O),

yet the two mainly overlap. Therefore, by reducing air pollution, we are protecting the climate. Studies such as that of Ding et al. (2009) have shown that climate change and air pollution share many common causes, i.e., both are primarily caused by emissions from fossil fuel combustion. For example, air pollutants from diesel engines travel around the globe as suspended particles, eventually reaching incredibly remote places, including polar regions. When pollutants cling to snow and ice, the color of the snow and ice darkens slightly, causing less sunlight to be reflected into space, thus contributing to the Earth's greenhouse effect. Slightly warmer temperatures also allow plants in sub-Arctic regions to grow slightly thicker, and the area of shadow they cast in the snow expands. If millions of small plants followed this growth pattern, the overall effect would double, and the entire surface would become darker, leading to a further increase in global warming. Also, reducing emissions of some high-impact, short-lived climate pollutants - such as methane, tropospheric ozone, HFCs, and black carbon - can significantly reduce the chances of triggering dangerous climate tipping points, such as the melting of Arctic permafrost, which releases carbon dioxide and methane irreversibly.

According to the Air Quality and Climate Bulletin published by WMO (World Meteorological Organization) in 2021, there is evidence of a strong relationship between air quality and climate change. Anthropogenic air pollutant emissions declined in 2020, but air quality is affected by dust storms and wildfires due to climate change (WMO, 2021). Climate change can affect the proportion, propagation, dispersion, and interactions among air pollutants. Regional climate changes, caused by climate directly and/or locally driven factors such as urbanization, can directly affect air quality. For example, regional climate change can reduce surface wind, directly leading to the aggregation of air pollutants and deterioration of air quality in the region.

Future research is planned to 1) focus on the impact of transboundary air pollution and urbanization on regional air quality under climate change, using the Japanese port city of Kitakyushu as an example of how the nature of its air quality affected will change under the impact of transboundary air pollution and urbanization; and 2) what kind of climate change will result if the government implements stricter policy control of air pollutants in the region.

References

Ding, Y.H., Li, Q.P., Liu, Y.J., Zhang, L., Song, Y.F., Zhang, J., 2009. Atmospheric Aerosols, Air Pollution and Climate Change. Meteorological Monthly, 35(3): 3-14. (in Chinese with English abstract).

World Meteorological Organization (WMO), WMO Air Quality and Climate Bulletin. No. 1, 2021. https://library.wmo.int/doc_num.php?explnum_id=10887.

Acknowledgements

First of all, I would like to thank academic supervisor Prof. Masahide Aikawa for his invaluable guidance and inspiration. Without his advice and guidance, this study could not have been completed. After his tiring and hectic daily work, Prof. Aikawa still devoted his considerate care and immense vigor to the supervision of writing the thesis, including his suggestions on wording, his help in forming the structure, and his refinement of ideas in this thesis. In addition, I must express sincere thanks to all the professors and teachers at The University of Kitakyushu for their enlightening courses and lectures during these three years of study.

I would like to express my thanks to my co-researchers; Ms. Miu Suzuki, Ms. Linh Khanh Nguyen, and Dr. Xi Zhang for their cooperation. I also extend my gratitude to all my partners in Aikawa's laboratory, Dr. Xi Zhang, Ms. Linh Khanh Nguyen, Mr. Duy Van Nguyen, and Mr. Dung Tran Nguyen, thanks for their assistance. A daily sampling at the University of Kitakyushu was carried out with the support of Mr. Kotaro Hirokawa and Mr. Takuya Murakami.

I would love to appreciate my parents, Xiaoping Peng and Wenxiu Yao, for their endless love and care for me. And my family members, Luyun Peng, Ling Tao, and Lin Hangwei have always given me support. Thanks to Hangwei Lin for encouraging and taking care in Japan. Whatever I need and wherever I go, they are always there supporting me without any requirement in return. I thank my loving family and family is where I can forever turn.

I also want to thank to all the people who help me, care about me and wish me for the best. The achievement of the thesis belongs to us, testifying our cooperation, our diligence, persistence and perpetual friendship.